

# Formation and evolution of compact stellar X-ray sources

T. M. Tauris  
Copenhagen University

E. P. J. van den Heuvel  
University of Amsterdam

## 16.1 Introduction and brief historical review

In this chapter we present an overview of the formation and evolution of compact stellar X-ray sources. For earlier reviews on the subject we refer to Bhattacharya & van den Heuvel (1991), van den Heuvel (1994) and Verbunt & van den Heuvel (1995). The observations and populations of high-mass X-ray binaries (HMXBs) and low-mass X-ray binaries (LMXBs) were covered earlier in Chapter 1 by Psaltis.

In our Galaxy there are about 100 bright X-ray sources with fluxes well above  $10^{-10}$  erg cm $^{-2}$  s $^{-1}$  in the energy range 1–10 keV (above the Earth's atmosphere). The distribution of these sources shows a clear concentration towards the Galactic center and also towards the Galactic plane, indicating that the majority do indeed belong to our Galaxy. Furthermore, a dozen strong sources are found in Galactic globular clusters (Section 8.2) and in the Magellanic Clouds. Shortly after the discovery of the first source (Sco X-1, Giacconi *et al.* 1962) Zel'Dovitch and Guseinov (1966), Novikov and Zel'Dovitch (1966) and Shklovskii (1967) suggested that the strong Galactic X-ray sources are accreting neutron stars or black holes in binary systems. (The process of mass accretion onto a supermassive black hole had already been suggested as the energy source for quasars and active galactic nuclei by Salpeter (1964), Zel'Dovitch (1964) and Zel'Dovitch and Novikov (1964).)

The X-ray fluxes measured correspond to typical source luminosities of  $10^{34} - 10^{38}$  erg s $^{-1}$  (which is more than 25 000 times the total energy output of our Sun). Table 16.1 lists the rates of accretion required to generate a typical X-ray luminosity of  $10^{37}$  erg s $^{-1}$ . Also listed is the amount of gravitational potential energy released per unit mass ( $\Delta U/m = GM/R$ ) by accretion onto a  $1 M_{\odot}$  stellar (compact) object, as well as the column density towards the stellar surface (or Schwarzschild radius) in the case of spherical accretion,  $\sigma = L_X 4\pi \sqrt{R/(GM)^3}$ . The table shows that only for accreting neutron stars and black holes is the column density low enough to allow X-rays to escape, as X-rays are stopped at column densities larger than a few g cm $^{-2}$ . Hence, the strongest Galactic sources cannot be accreting white dwarfs.

The first evidence for an accreting binary came from Webster and Murdin (1972) and Bolton (1972). They discovered that Cyg X-1 is a binary system with an orbital period of 5.6 days. They measured the amplitude of the radial velocity curve (72 km s $^{-1}$ ) of the O9.7 supergiant optical counterpart, and independently concluded that the X-ray emission is the result of accretion onto a compact object, which is probably a black hole given the fact that the derived mass of the compact object  $> 3 M_{\odot}$  when assuming a realistic mass ( $\geq 15 M_{\odot}$ ) for the O9.7 supergiant.

Table 16.1. *Energetics of accretion: see text*

Stellar object	Radius (km)	$\Delta U/mc^2$	$\Delta U/m$ (erg/g)	$dM/dt^a$ ( $M_\odot/\text{yr}$ )	Column density <sup>a</sup> ( $\text{g}/\text{cm}^2$ )
Sun	$7 \times 10^5$	$2 \times 10^{-6}$	$2 \times 10^{15}$	$1 \times 10^{-4}$	140
White dwarf	10 000	$2 \times 10^{-4}$	$1 \times 10^{17}$	$1 \times 10^{-6}$	16
Neutron star	10	0.15	$1 \times 10^{20}$	$1 \times 10^{-9}$	0.5
Black hole	3	0.1 ~ 0.4	$4 \times 10^{20}$	$4 \times 10^{-10}$	0.3

<sup>a</sup>  $L_X = 10^{37}$  erg/s

Shortly afterwards, the accreting binary model was nicely confirmed by Schreier *et al.* (1972) who discovered that the regularly pulsing source Cen X-3 is a member of an eclipsing binary system. Its regular X-ray pulsations (indicating a neutron star) have a period of 4.84 s, and the regular X-ray eclipses have a duration of 0.488 days, and repeat every 2.087 days. The pulse period shows a sinusoidal Doppler modulation with the same 2.087 day period and is in phase with the X-ray eclipses, indicating that the X-ray pulsar is moving in a circular orbit with a projected velocity of 415.1 km s<sup>-1</sup>. Hence, the 4.84 s period of the X-ray pulsations is the rotation period of the neutron star and the binary orbital period is 2.087 days. Using Kepler's third law ( $\Omega^2 = GM/a^3$ ) combined with the eccentricity and measured radial velocity amplitude ( $K_x = \Omega a_x \sin i / \sqrt{1 - e^2}$ ) of the X-ray pulsar one can determine the so-called mass function of the binary:

$$f(M) = \frac{M_2^3 \sin^3 i}{(M_X + M_2)^2} = \frac{1}{2\pi G} K_x^3 P_{\text{orb}} (1 - e^2)^{3/2} \quad (16.1)$$

where  $M_X$  and  $M_2$  denote the masses of the accreting compact star and its companion star, respectively, and  $i$  is the inclination of the orbital angular momentum vector with respect to the line-of-sight to the Earth. For Cen X-3 the mass function is  $f = 15.5 M_\odot$  and thus one can derive a minimum companion mass of about  $18 M_\odot$ .

The recognition that neutron stars and black holes can exist in close binary systems came at first as a surprise. It was known that the initially more massive star should evolve first and explode in a supernova (SN). However, as a simple consequence of the virial theorem, the orbit of the post-SN system should be disrupted if more than half of the total mass of the binary is suddenly ejected (Blaauw 1961). For X-ray binaries like Cen X-3 it was soon realized (van den Heuvel & Heise 1972; and independently also by Tutukov & Yungelson 1973) that the survival of this system was due to the effects of large-scale mass transfer that must have occurred prior to the SN.

The formation of low-mass X-ray binaries ( $M_{\text{donor}} \leq 1.5 M_\odot$ ) with observed orbital periods mostly between 11 min and 12 hr, as well as the discovery of the double neutron star system PSR 1913+16 (Hulse & Taylor 1975) with an orbital period of 7.75 hr, was a much tougher nut to crack. How could these stars end up being so close when the progenitor star of the neutron star must have had a radius much larger than the current separation? It was clear that such systems must have lost a large amount of orbital angular momentum. The first models to include large loss of angular momentum were made by van den Heuvel and de Loore (1973) for the later evolution of high-mass X-ray binaries (HMXBs), showing that

in this way very close systems like Cyg X-3 can be formed, and Sutantyo (1975) for the origin of LMXBs. The important concept of a “common envelope” (CE) evolution was introduced by Paczyński (1976) and Ostriker (1976). This scenario, as well as that of van den Heuvel and de Loore (1973), could link the massive X-ray binary Cyg X-3 and the binary radio pulsar PSR 1913+16. In this scenario a neutron star is captured by the expansion of a giant companion star and is forced to move through the giant’s envelope. The resulting frictional drag will cause its orbit to shrink rapidly while, at the same time, ejecting the envelope before the naked core of the giant star explodes to form another neutron star. It was suggested by Smarr and Blandford (1976) that it is an old “spun-up” neutron star which is observed as a radio pulsar in PSR 1913+16. The magnetic field of this visible pulsar is relatively weak ( $\sim 10^{10}$  G, some two orders of magnitude lower than the average pulsar magnetic field) and its spin period is very short (59 ms). Hence, this pulsar is most likely spun-up (or “recycled”) in an X-ray binary where mass and angular momentum from an accretion disk is fed to the neutron star (as already suggested by Bisnovatyi-Kogan and Komberg 1974). The other neutron star in the system was then produced by the second supernova explosion and must be a young, strong **B**-field neutron star (it is not observable – either because it has already rapidly spun-down, due to dipole radiation, or because the Earth is not hit by the pulsar beam).

The idea of recycling pulsars was given a boost by the discovery of the first millisecond radio pulsar (Backer *et al.* 1982). As a result of the long accretion phase in LMXBs, millisecond pulsars are believed to be formed in such systems (Alpar *et al.* 1982; Radhakrishnan & Srinivasan 1982). This model was beautifully confirmed by the discovery of the first millisecond X-ray pulsar in the LMXB system SAX 1808.4–3658 (Wijnands & van der Klis 1998). Now four of these accreting millisecond pulsars are known (Galloway *et al.* 2002; Markwardt, Smith & Swank 2003). For a detailed discussion on the evidence for the presence of rapidly spinning weakly magnetized neutron stars in low-mass X-ray binaries we refer to Chapter 2 by van der Klis and Chapter 3 by Strohmayer and Bildsten.

Finally, another ingredient that has important consequences for close binary evolution is the event of a “kick” imparted to newborn neutron stars as a result of an asymmetric SN. They were first applied to binary systems by Flannery and van den Heuvel (1975). There is now ample evidence for the occurrence of such kicks inferred from the space velocities of pulsars and from dynamical effects on surviving binaries (e.g., Dewey & Cordes 1987; Lyne & Lorimer 1994 and Kaspi *et al.* 1996). Furthermore, as argued by Kalogera and Webbink (1998), without kicks the formation of LMXBs with short orbital periods cannot be explained.

In this review we will concentrate on the stellar evolutionary processes that are responsible for the formation of the different types of compact binaries and their evolution. Our focus is mainly on binaries with neutron star or black hole accretors. We refer to other reviews for discussions on CVs and AM CVn systems (Chapter 10), super-soft sources (Chapter 11) and sdB-star binaries (Maxted *et al.* 2001; Han *et al.* 2002). In the next section, however, we will first give a short introduction to the observational properties of the X-ray binaries and binary pulsars which we discuss afterwards (see also Chapter 1 by Psaltis).

## 16.2 Compact binaries and their observational properties

Over 90% of the strong Galactic X-ray sources appear to fall into two distinct groups: the high-mass X-ray binaries (HMXBs) and the low-mass X-ray binaries (LMXBs). These

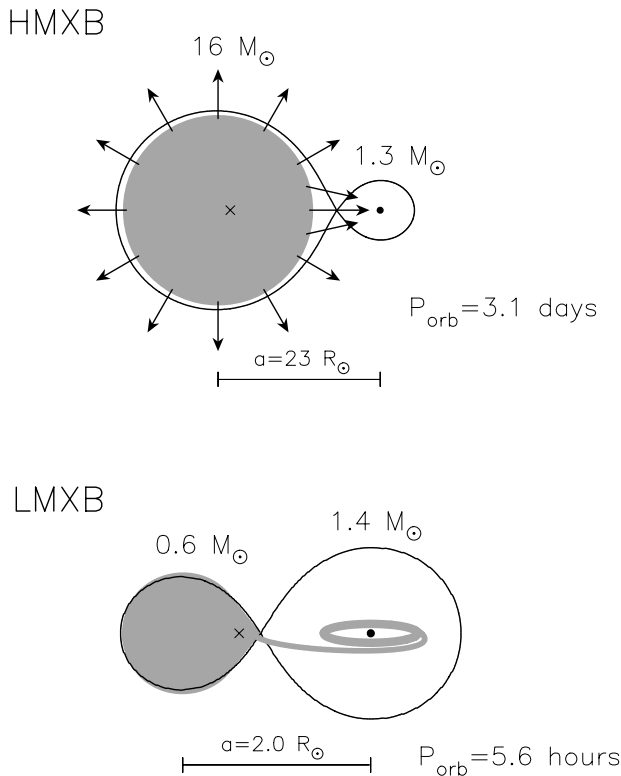


Fig. 16.1. Examples of a typical HMXB (*top*) and LMXB (*bottom*). The neutron star in the HMXB is fed by a strong high-velocity stellar wind and/or by beginning atmospheric Roche-lobe overflow. The neutron star in an LMXB is surrounded by an accretion disk which is fed by Roche-lobe overflow. There is also observational evidence for HMXBs and LMXBs harboring black holes.

two groups differ in a number of physical characteristics (see Fig. 16.1 and Table 16.2 for some examples). As we shall see later on, binary pulsars and single millisecond pulsars are the descendants of the X-ray binaries containing an accreting neutron star.

### 16.2.1 High-mass X-ray binaries (HMXBs)

There are about 130 known HMXBs (Liu, van Paradijs & van den Heuvel 2000) and 25 have well-measured orbital parameters. There are  $\sim 40$  pulsating HMXB sources with typical pulse periods between 10 and 300 seconds (the entire observed range spans between 0.069 seconds and 20 minutes). Among the systems with  $P_{\text{orb}} \leq 10$  days and  $e \leq 0.1$  are the strong sources and “standard” systems such as Cen X-3 and SMC X-1. These are characterized by the occurrence of regular X-ray eclipses and double-wave ellipsoidal light variations produced by tidally deformed (“pear-shaped”) giant or sub-giant companion stars with masses  $> 10 M_{\odot}$ . However, the optical luminosities ( $L_{\text{opt}} > 10^5 L_{\odot}$ ) and spectral types of the companions indicate original ZAMS masses  $\geq 20 M_{\odot}$ , corresponding to O-type progenitors. The companions have radii  $10\text{--}30 R_{\odot}$  and (almost) fill their critical Roche-lobes, see Section 16.4. In a number of pulsating sources, such as X0115+63 (and Her X-1, an intermediate-mass X-ray binary system) there are absorption/emission features in the

Table 16.2. The two main classes of strong Galactic X-ray sources

	HMXB	LMXB
X-ray spectra	$kT \geq 15$ keV (hard)	$kT \leq 10$ keV (soft)
Type of time variability	regular X-ray pulsations no X-ray bursts	only a very few pulsars often X-ray bursts
Accretion process	wind (or atmos. RLO)	Roche-lobe overflow
Timescale of accretion	$10^5$ yr	$10^7 - 10^9$ yr
Accreting compact star	high <b>B</b> -field NS (or BH)	low <b>B</b> -field NS (or BH)
Spatial distribution	Galactic plane	Galactic center and spread around the plane
Stellar population	young, age $< 10^7$ yr	old, age $> 10^9$ yr
Companion stars	luminous, $L_{\text{opt}}/L_X > 1$ early-type O(B)-stars $> 10 M_{\odot}$ (Pop. I)	faint, $L_{\text{opt}}/L_X \ll 0.1$ blue optical counterparts $\leq 1 M_{\odot}$ (Pop. I and II)

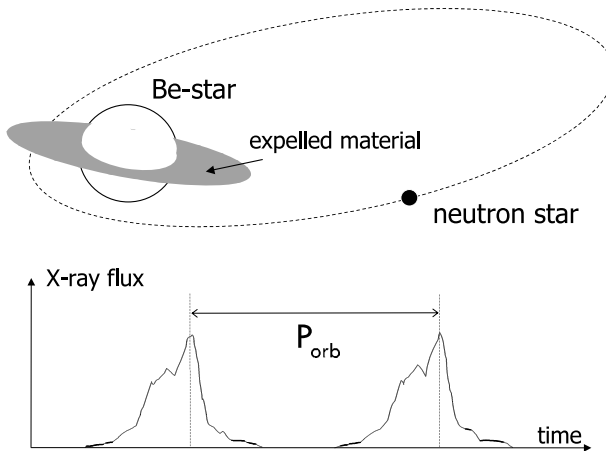


Fig. 16.2. Schematic model of a Be-star X-ray binary system. The neutron star moves in an eccentric orbit around the Be-star which is not filling its Roche-lobe. However, near the periastron passage the neutron star accretes circumstellar matter, ejected from the rotating Be-star, resulting in an X-ray outburst lasting several days.

X-ray spectrum that are most probably cyclotron lines, resulting from magnetic fields with strengths  $B \simeq 5 \times 10^{12}$  G (Kirk & Trümper 1983). Among the standard HMXBs, there are at least two systems that are thought to harbor black holes: Cyg X-1 and LMC X-3.

Another group of HMXBs consists of the moderately wide, eccentric binaries with  $P_{\text{orb}} \simeq 20 - 100$  days and  $e \simeq 0.3 - 0.5$ . A new third (sub-)group has recently been proposed by Pfahl *et al.* (2002). These systems have  $P_{\text{orb}} \simeq 30 - 250$  days and small eccentricities  $e \lesssim 0.2$ . Together these two groups form a separate sub-class of HMXBs: the Be-star X-ray binaries (see Fig. 16.2; first recognized as a class by Maraschi, Treves & van den Heuvel 1976). In the Be-star X-ray binaries the companions are rapidly rotating B-emission stars situated on, or close to, the main sequence (luminosity class III–V). There are more than 50 such systems

known making them the most numerous class of HMXBs (see, for example, van den Heuvel & Rappaport 1987 and Chapter 1 by Psaltis for reviews). The Be-stars are deep inside their Roche-lobes, as is indicated by their generally long orbital periods ( $\gtrsim 15$  days) and by the absence of X-ray eclipses and of ellipsoidal light variations. According to the luminosities and spectral types, the companion stars have masses in the range about 8–20  $M_{\odot}$  (spectral types O9–B3, III–V). The X-ray emission from the Be-star X-ray systems tends to be extremely variable, ranging from complete absence to giant transient outbursts lasting weeks to months. During such an outburst episode one often observes orbital modulation of the X-ray emission, due to the motion of the neutron star in an eccentric orbit, see Fig. 16.2. The recurrent X-ray outbursts are most probably related to the irregular optical outbursts generally observed in Be-stars, which indicate sudden outbursts of mass ejection, presumably generated by rotation-driven instability in the equatorial regions of these stars (see, for example, Slettebak 1988). While the Be-star X-ray binaries are transient sources (often unobservable for months to years) the “standard” systems are persistent X-ray sources. HMXBs are located along the Galactic plane among their OB-type progenitor stars.

### 16.2.2 *Low-mass X-ray binaries (LMXBs)*

Orbital periods have been measured for some 30 of these systems. They range from 11 minutes to 17 days, similar to the orbital periods of cataclysmic variables – see also Chapter 5 by Charles and Coe. Only in the widest few of these systems can one observe the spectrum of the optical companion. In all other systems, the optical spectrum is that of the hot accretion disk. The LMXBs are very seldom X-ray pulsars. The reason is their relatively weak magnetic fields  $\sim 10^9$ – $10^{11}$  G, which are expected to result from accretion-induced field decay (Taam & van den Heuvel 1986; Geppert & Urpin 1994; Konar & Bhattacharya 1997; Cumming, Zweibel & Bildsten 2001; Bhattacharya 2002). On the other hand, these sources show X-ray bursts (sudden thermonuclear fusion of accreted matter at the surface of the neutron star – see Chapter 3 by Strohmayer and Bildsten), which are suppressed if the magnetic field strength  $> 10^{11}$  G (Lewin & Joss 1983). For this reason such bursts are not observed in HMXBs. The discovery of (kilohertz) quasi-periodic oscillations (QPOs) in the X-ray flux of LMXBs has provided a clear timing signature of the accreting neutron stars and black holes in these systems. In the past decade much insight of detailed accretion physics and testing of the general theory of relativity has been revealed by observations and “beat frequency” models (see Chapter 2 by van der Klis for a review). There are more than a dozen LMXBs systems for which there is strong evidence for the presence of a black hole – see Section 16.2.4 and Chapters 4 and 5.

Most of the LMXBs are located in the Galactic bulge and in globular clusters, and thus appear to belong to an old stellar population. They do not show considerable run-away characteristics, as they are confined mostly to within 0.6 kpc of the Galactic plane – however, some LMXBs have transverse velocities in excess of 100  $\text{km s}^{-1}$ . It is interesting to notice that the systems in globular clusters must have velocities smaller than the escape velocities from these clusters, which are less than about 30  $\text{km s}^{-1}$ .

### 16.2.3 *Intermediate-mass X-ray binaries (IMXBs)*

Above we have described the HMXB and LMXB systems with companion stars  $> 10 M_{\odot}$  and  $\lesssim 1 M_{\odot}$ , respectively. There must also exist a large number of Galactic compact

binaries with companion star masses in the interval  $1\text{--}10 M_{\odot}$  as has been argued, e.g., by van den Heuvel (1975). These are the so-called intermediate-mass X-ray binaries (IMXBs). IMXBs have recently been recognized as a class of their own. It is important to be aware that IMXB systems are not easily observed as a result of a simple selection effect against X-ray sources with intermediate-mass companions. The reason is the following (van den Heuvel 1975): “Standard” HMXBs have evolved (sub)giant companions that are massive enough to have a strong stellar wind mass-loss rate (typically  $\dot{M}_{\text{wind}} \simeq 10^{-6} M_{\odot} \text{ yr}^{-1}$ ) sufficient to power a bright X-ray source, via an accreting neutron star or black hole, for  $10^5\text{--}10^6$  yr. The LMXBs are not wind-fed X-ray sources. These systems experience mass transfer via Roche-lobe overflow (RLO) from their companion star to the compact object. The LMXBs often evolve slowly on a nuclear timescale ( $\sim 10^8\text{--}10^9$  yr) and the majority of the transferred material is usually funneled onto the compact object, via an accretion disk, yielding accretion rates of  $10^{-10}\text{--}10^{-8} M_{\odot} \text{ yr}^{-1}$ . In IMXBs the companions are not massive enough to produce sufficiently high wind mass-loss rates to power an observable X-ray source. Subsequently when IMXBs evolve through RLO, the relatively large mass ratio between the companion star and a neutron star causes this phase to be short lived – either on a sub-thermal timescale (Tauris, van den Heuvel & Savonije 2000), or the system evolves through a common envelope. In either case, the systems evolve on a timescale of only a few 1000 yr. Furthermore, the very high mass-transfer rates under these circumstances ( $\dot{M} > 10^{-4} M_{\odot} \text{ yr}^{-1} \gg \dot{M}_{\text{Edd}}$ ) may cause the emitted X-rays to be absorbed in the dense gas surrounding the accreting neutron star. We therefore conclude that HMXBs and LMXBs are naturally selected as persistent X-ray sources fed by a strong stellar wind and RLO, respectively.

Also, from a theoretical point of view we know that IMXBs must exist in order to explain the formation of binary pulsars with heavy CO or ONeMg white dwarf companions (Tauris, van den Heuvel & Savonije 2000). Despite the above mentioned selection effects against IMXBs there are a few such systems with neutron stars detected: Her X-1 and Cyg X-2 are systems of this type. In the latter system the companion presently has a mass of  $< 1 M_{\odot}$ , but it is highly over-luminous for this mass, which indicates that it is an evolved star that started out with a mass between 3 and  $4 M_{\odot}$  at the onset of the mass-transfer phase (Podsiadlowski & Rappaport 2000; King & Ritter 1999). Among the black hole X-ray binaries, IMXBs are more common, for example: GRO J1655–40 ( $M_{\text{d}} \sim 1.5 M_{\odot}$ ; Beer & Podsiadlowski 2002), 4U 1543–47 ( $M_{\text{d}} \sim 2.5 M_{\odot}$ ; Orosz *et al.* 1998), LMC X-3 ( $M_{\text{d}} \sim 5 M_{\odot}$ ; Soria *et al.* 2001) and V 4642 Sgr ( $M_{\text{d}} \sim 6.5 M_{\odot}$ ; Orosz *et al.* 2001). In these systems the donor star ( $M_{\text{d}}$ ) is less massive than the black hole, so mass transfer by RLO is stable.

#### 16.2.4 Soft X-ray transients (SXTs)

A great breakthrough in the discovery of black holes in X-ray binaries came with the discovery by McClintock and Remillard (1986) that the K5V companion of the source A0620–00, in a spectroscopic binary with  $P_{\text{orb}} = 7.75$  hr, has a velocity amplitude of  $> 470 \text{ km s}^{-1}$ . This large orbital velocity indicates that even if the K-dwarf had zero mass, the compact object would have mass of  $> 3 M_{\odot}$  and therefore must be a black hole. Since then over a dozen such systems consisting of a black hole with a low-mass donor star have been discovered. These black hole systems are the so-called soft X-ray transients (SXT) and appear as bright X-ray novae with luminosities  $L_{\text{X}} \sim 10^{38} \text{ erg s}^{-1}$  for several weeks. At

the same time, the optical luminosity of these systems brightens by 6 to 10 magnitudes, making them optical novae as well. After the decay of the X-ray and optical emission, the spectrum of a K or G star becomes visible, and the large amplitude variations ( $\geq 100 \text{ km s}^{-1}$ ) in the radial velocities of these stars indicate a compact object mass of  $> 3 M_{\odot}$  (exceeding the maximum mass thought possible for neutron stars). Their orbital periods are between 8 hours and 6.5 days (see e.g., Lee, Brown & Wijers 2002 and Chapter 4 by McClintock & Remillard).

### 16.2.5 Peculiar X-ray binaries

Not all observed X-ray binaries fall into the well-defined classes described above. Among the more intriguing systems are SS433 and Cyg X-3, which both have flaring radio emissions and jets (see, e.g., Chapter 9 by Fender). Cyg X-3 ( $P_{\text{orb}} = 4.8 \text{ hr}$ ) is probably a later evolutionary phase of a wide HMXB (e.g., see Fig. 16.15 in Section 16.8; van den Heuvel & de Loore 1973).

### 16.2.6 The binary and millisecond radio pulsars

The 50 or so Galactic binary radio pulsars detected so far are generally characterized by short spin periods,  $P$ , and small values of the period derivative,  $\dot{P}$ . This can clearly be seen in a  $(P, \dot{P})$ -diagram of radio pulsars, see Fig. 16.3. Simple expressions for the surface magnetic dipole field strength,  $B$ , and “spin-down” age,  $\tau$ , are given by the magnetic dipole model of pulsars (see Manchester & Taylor 1977):

$$B = \sqrt{\frac{3c^3 I}{8\pi^2 R^6} P \dot{P}} \simeq 3 \times 10^{19} \sqrt{P \dot{P}} \text{ gauss} \quad (16.2)$$

where  $I$  and  $R$  are the moment of inertia ( $\sim 10^{45} \text{ g cm}^2$ ) and radius of the neutron star, respectively, and

$$\tau \equiv P/2\dot{P} \quad (16.3)$$

Figure 16.3 shows that the binary pulsars typically have  $B = 10^8 - 10^{10} \text{ G}$  and  $\tau = 1 - 10 \text{ Gyr}$ , whereas the ordinary isolated pulsars have  $B = 10^{12} - 10^{13} \text{ G}$  and  $\tau \lesssim 10 \text{ Myr}$ . As will be discussed in a later section in this chapter, the short spin periods and low values of  $B$  are consequences of the recycling process where an old neutron star accretes mass and angular momentum from its companion star via an accretion disk. For theoretical calculations of the dynamical evolution of single pulsars in the  $(P, \dot{P})$ -diagram we refer to Tauris & Konar (2001).

There are four classes of binary pulsars detected so far (see Table 16.3). The different classes are: (i) high-mass binary pulsars (HMBPs) with a neutron star or ONeMg/CO white dwarf companion, (ii) low-mass binary pulsars (LMBPs) with a helium white dwarf companion, (iii) non-recycled pulsars with a CO white dwarf companion, and finally, (iv) pulsars with an unevolved companion. A few further sub-divisions can be introduced from an evolutionary point of view. The globular cluster pulsars will not be discussed here since these systems are the result of tidal capture or exchange encounters – see Bhattacharya & van den Heuvel (1991) and Chapter 8 by Verbunt & Lewin for a review.

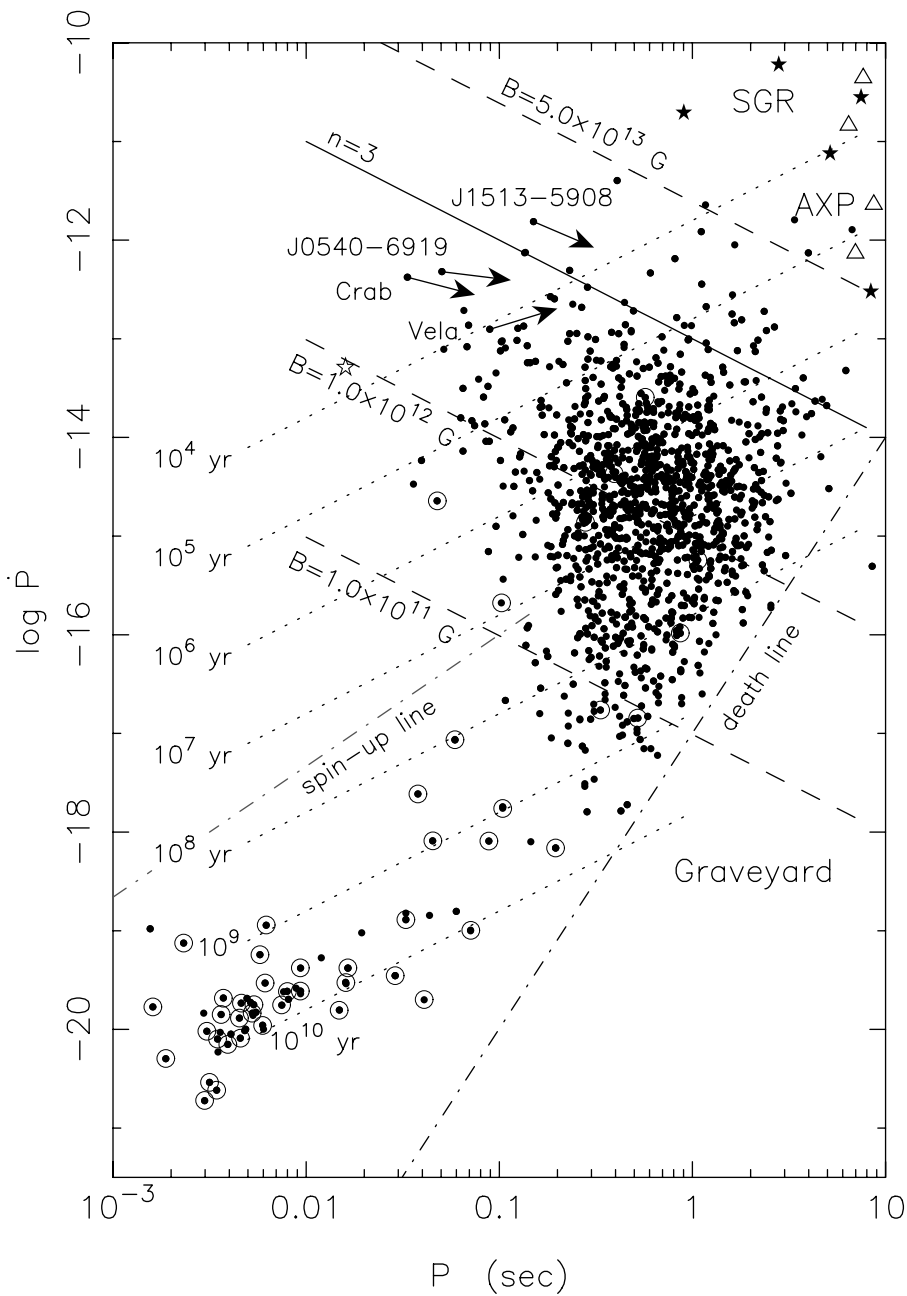


Fig. 16.3. ( $P, \dot{P}$ )-diagram of  $\sim 1300$  observed radio pulsars (ATNF Pulsar Catalogue data). Binary pulsars are marked by a circle. Soft gamma-ray repeaters (SGR) and anomalous X-ray (AXP) pulsars (Chapter 14) are marked by stars and triangles, respectively. Also shown are lines of constant surface dipole magnetic field strength (dashed) and characteristic ages (dotted). The arrows marked on a few young pulsars indicate a measurement of the braking index. The “death line” is the pair-creation limit for generating radio pulses.

Table 16.3. *Main categories and types of binaries with compact objects*

Main type	Sub-type	Observed example	$P_{\text{orb}}$
<i>X-ray binaries</i>			
high-mass donor ( $M_{\text{donor}} \geq 10 M_{\odot}$ )	“standard” HMXB	Cen X-3 Cyg X-1	2.087 <sup>d</sup> (NS) 5.60 <sup>d</sup> (BH)
	wide-orbit HMXB	X Per	250 <sup>d</sup> (NS)
	Be-star HMXB	A0535+26	104 <sup>d</sup> (NS)
	low-mass donor ( $M_{\text{donor}} \leq 1 M_{\odot}$ )	Galactic disk LMXB	Sco X-1
low-mass donor ( $M_{\text{donor}} \leq 1 M_{\odot}$ )	soft X-ray transient	A0620–00	7.75 <sup>hr</sup> (BH)
	globular cluster	X 1820–30	11 <sup>min</sup> (NS)
	millisecond X-ray pulsar	SAX J1808.4–36	2.0 <sup>d</sup> (NS)
intermediate-mass donor ( $1 < M_{\text{donor}}/M_{\odot} < 10$ )		Her X-1	1.7 <sup>d</sup> (NS)
		Cyg X-2	9.8 <sup>d</sup> (NS)
		V 404 Cyg	6.5 <sup>d</sup> (BH)
<i>Binary radio pulsars</i>			
“high-mass” companion ( $0.5 \leq M_c/M_{\odot} \leq 1.4$ )	NS + NS (double)	PSR 1913+16	7.75 <sup>hr</sup>
	NS + (ONeMg) WD	PSR 1435–6100	1.35 <sup>d</sup>
	NS + (CO) WD	PSR 2145–0750	6.84 <sup>d</sup>
“low-mass” companion ( $M_c < 0.45 M_{\odot}$ )	NS + (He) WD	PSR 0437–4715	5.74 <sup>d</sup>
		PSR 1640+2224	175 <sup>d</sup>
non-recycled pulsar unevolved companion	(CO) WD + NS	PSR 2303+46	12.3 <sup>d</sup>
	B-type companion	PSR 1259–63	3.4 <sup>yr</sup>
	low-mass companion	PSR 1820–11	357 <sup>d</sup>
<i>CV-like binaries</i>			
novae-like systems	( $M_{\text{donor}} \leq M_{\text{WD}}$ )	DQ Her	4.7 <sup>hr</sup>
		SS Cyg	6.6 <sup>hr</sup>
super-soft X-ray sources	( $M_{\text{donor}} > M_{\text{WD}}$ )	CAL 83	1.04 <sup>d</sup>
		CAL 87	10.6 <sup>hr</sup>
AM CVn systems (RLO)	(CO) WD + (He) WD	AM CVn	22 <sup>min</sup>
double WD (no RLO)	(CO) WD + (CO) WD	WD1204+450	1.6 <sup>d</sup>
sdB-star systems	(sdB) He-star + WD	KPD 0422+5421	2.16 <sup>hr</sup>

### 16.3 Binary stellar evolution and final compact objects

In order to understand how neutron stars, black holes and white dwarfs can be formed in binary systems, a brief overview of the basic elements of the evolution of single stars is necessary. We refer to, e.g., Cox & Giuli (1968) and Kippenhahn & Weigert (1990) for further details.

#### 16.3.1 Summary of the evolution of single stars

The evolution of a star is driven by a rather curious property of a self-gravitating gas in hydrostatic equilibrium, described by the virial theorem, namely that the radiative loss of energy of such a gas causes it to contract and hence, due to release of gravitational potential energy, to increase its temperature. Thus, while the star tries to cool itself by radiating away energy from its surface, it gets hotter instead of cooler (i.e., it has a “negative heat capacity”).

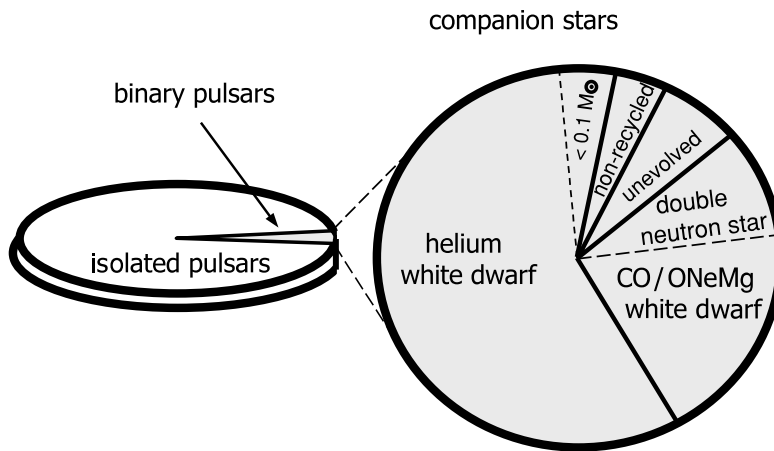


Fig. 16.4. Illustration of the relative distribution of all  $\sim 1500$  radio pulsars observed. About 4% are members of a binary system. The four main classes of binary pulsars are defined according to their formation history – see text.

The more it radiates to cool itself, the more it will contract, the hotter it gets and the more it is forced to go on radiating. Clearly, this “vicious virial cycle” is an unstable situation in the long run and explains why the star, starting out as an interstellar gas globe, must finally end its life as a compact object. In the meantime the star spends a considerable amount of time in the intermediate stages, which are called: “the main sequence”, “the giant branch”, etc. It is important to realize that stars do *not* shine because they are burning nuclear fuel. They shine because they are hot due to their history of gravitational contraction.

A massive star ( $M \gtrsim 10 M_{\odot}$ ) evolves through cycles of nuclear burning alternating with stages of exhaustion of nuclear fuel in the stellar core until its core is made of iron, at which point further fusion requires, rather than releases, energy. The core mass of such a star becomes larger than the Chandrasekhar limit, the maximum mass possible for an electron-degenerate configuration ( $\sim 1.4 M_{\odot}$ ). Therefore the core implodes to form a neutron star or black hole. The gravitational energy released in this implosion ( $4 \times 10^{53}$  erg  $\simeq 0.15 M_{\text{core}} c^2$ ) is far more than the binding energy of the stellar envelope, causing the collapsing star to explode violently and eject the outer layers of the star, with a speed of  $\sim 10^4$  km s $^{-1}$ , in a supernova event. The final stages during and beyond carbon burning are very short-lived ( $\sim 60$  yr for a  $25 M_{\odot}$  star) because most of the nuclear energy generated in the interior is liberated in the form of neutrinos, which freely escape without interaction with the stellar gas, thereby lowering the outward pressure and accelerating the contraction and nuclear burning.

Less massive stars ( $M < 8 M_{\odot}$ ) suffer from the occurrence of degeneracy in the core at a certain point of evolution. Since for a degenerate gas the pressure only depends on density and not on temperature, there will be no stabilizing expansion and subsequent cooling after the ignition. Hence, the sudden temperature rise (due to the liberation of energy after ignition) causes run-away nuclear energy generation producing a so-called “flash”. In stars with  $M < 2.3 M_{\odot}$  the helium core becomes degenerate during hydrogen shell burning and, when its core mass  $M_{\text{He}}$  reaches  $0.45 M_{\odot}$ , helium ignites with a flash. The helium flash is, however, not violent enough to disrupt the star. Stars with masses in the range  $2.3 < M/M_{\odot} < 8$  ignite carbon with a flash. Such a carbon flash was believed to perhaps disrupt the entire star in a so-called carbon-deflagration supernova. However, recent observations of white dwarfs in

Table 16.4. *End products of stellar evolution as a function of initial mass*

Initial mass	He-core mass	Final product	
		Single star	Binary star
$< 2.3 M_{\odot}$	$< 0.45 M_{\odot}$	CO white dwarf	He white dwarf
$2.3 - 6 M_{\odot}$	$0.5 - 1.9 M_{\odot}$	CO white dwarf	CO white dwarf
$6 - 8 M_{\odot}$	$1.9 - 2.1 M_{\odot}$	O-Ne-Mg white dwarf or C-deflagration SN?	O-Ne-Mg white dwarf
$8 - 12 M_{\odot}$	$2.1 - 2.8 M_{\odot}$	neutron star	O-Ne-Mg white dwarf
$12 - 25 M_{\odot}$	$2.8 - 8 M_{\odot}$	neutron star	neutron star
$> 25 M_{\odot}$	$> 8 M_{\odot}$	black hole	black hole

Galactic clusters that still contain stars as massive as  $8_{-2}^{+3} M_{\odot}$  (Reimers & Koester 1988; Weidemann 1990) indicate that such massive stars still terminate their life as a white dwarf. They apparently shed their envelopes in the AGB-phase before carbon ignites violently. Furthermore, stars in close binary systems, which are the prime objects in this review, will have lost their envelope as a result of mass transfer via Roche-lobe overflow. This is also the reason why in binary systems the lower ZAMS mass-limit for producing a neutron star is somewhat larger than for an isolated star.

The possible end-products and corresponding initial masses are listed in Table 16.4. It should be noted that the actual values of the different mass ranges are only known approximately due to considerable uncertainty in our knowledge of the evolution of massive stars. Prime causes of this uncertainty include limited understanding of the mass loss undergone by stars in their various evolutionary stages (see Section 16.3.3). To make a black hole, the initial ZAMS stellar mass must exceed at least  $20 M_{\odot}$  (Fryer 1999), or possibly  $25 M_{\odot}$ . According to MacFadyen, Woosley and Heger (2001), stars  $> 40 M_{\odot}$  form black holes directly (collapsars type I) whereas stars in the interval  $25 < M/M_{\odot} < 40$  produce black holes after a “failed supernova explosion” (collapsars type II). From an analysis of black hole binaries it seems that a mass-fraction of  $\sim 0.35$  must have been ejected in the (symmetric) stellar core collapse leading to the formation of a black hole (Nelemans, Tauris & van den Heuvel 1999). Another fundamental problem is understanding convection, in particular in stars that consist of layers with very different chemical composition. Finally, there is the unsolved question of whether or not the velocity of convective gas cells may carry them beyond the boundary of the region of the star that is convective according to the Schwarzschild criterion. For example, inclusion of this so-called overshooting in evolutionary calculations decreases the lower mass-limit for neutron star progenitors.

### 16.3.1.1 Three timescales of stellar evolution

There are three fundamental timescales of stellar evolution. When the hydrostatic equilibrium of a star is disturbed (e.g., because of sudden mass loss), the star will restore this equilibrium on a so-called dynamical (or pulsational) timescale:

$$\tau_{\text{dyn}} = \sqrt{R^3/GM} \simeq 50 \text{ min } (R/R_{\odot})^{3/2} (M/M_{\odot})^{-1/2} \quad (16.4)$$

When the thermal equilibrium of a star is disturbed, it will restore this equilibrium on a thermal (or Kelvin–Helmholtz) timescale, which is the time it takes to emit all of its thermal

energy content at its present luminosity:

$$\tau_{\text{th}} = GM^2/RL \simeq 30 \text{ Myr } (M/M_{\odot})^{-2} \quad (16.5)$$

The third stellar timescale is the nuclear one, which is the time needed for the star to exhaust its nuclear fuel reserve (which is proportional to  $M$ ), at its present fuel consumption rate (which is proportional to  $L$ ), so this timescale is given by

$$\tau_{\text{nuc}} \simeq 10 \text{ Gyr } (M/M_{\odot})^{-2.5} \quad (16.6)$$

In calculating the above mentioned timescales we have assumed a mass–luminosity relation:  $L \propto M^{3.5}$  and a mass–radius relation for main-sequence stars:  $R \propto M^{0.5}$ . Both of these relations are fairly good approximations for  $M \geq M_{\odot}$ . Hence, it should also be noted that the rough numerical estimates of these timescales only apply to ZAMS stars.

### 16.3.2 The variation of the outer radius during stellar evolution

Figure 16.5 depicts the evolutionary tracks in the Hertzsprung–Russell diagram of six different stars (50, 20, 12, 5, 2 and 1  $M_{\odot}$ ). We calculated these tracks using Eggleton’s evolutionary code (e.g., Pols *et al.* 1995, 1998). The observable stellar parameters are: luminosity ( $L$ ), radius ( $R$ ) and effective surface temperature ( $T_{\text{eff}}$ ). Their well-known relationship is given by  $L = 4\pi R^2 \sigma T_{\text{eff}}^4$ . In Fig. 16.6 we have plotted our calculation of stellar radius as a function of age for the 5  $M_{\odot}$  star. Important evolutionary stages are indicated in the figures. Between points 1 and 2 the star is in the long-lasting phase of core hydrogen burning (nuclear timescale). At point 3 hydrogen ignites in a shell around the helium core. For stars more massive than 1.2  $M_{\odot}$  the entire star briefly contracts between points 2 and 3, causing its central temperature to rise. When the central temperature reaches  $\sim 10^8$  K, core helium ignites (point 4). At this moment the star has become a red giant, with a dense core and a very large radius. During helium burning it describes a loop in the H-R diagram. Stars with  $M \geq 2.3 M_{\odot}$  move from points 2 to 4 on a thermal timescale and describe the helium-burning loop on a (helium) nuclear timescale following point 4. Finally, during helium shell burning the outer radius expands again and at carbon ignition the star has become a red supergiant on the asymptotic giant branch (AGB).

The evolution of less massive stars ( $M < 2.3 M_{\odot}$ ) takes a somewhat different course. After hydrogen shell ignition the helium core becomes degenerate and the hydrogen burning shell generates the entire stellar luminosity. While its core mass grows, the star gradually climbs upwards along the red giant branch until it reaches helium ignition with a flash. For all stars less massive than about 2.3  $M_{\odot}$  the helium core has a mass of about 0.45  $M_{\odot}$  at helium flash ignition. The evolution described above depends only slightly on the initial chemical composition and effects of convective overshooting.

#### 16.3.2.1 The core mass–radius relation for low-mass RGB stars

For a low-mass star ( $\lesssim 2.3 M_{\odot}$ ) on the red giant branch (RGB) the growth in core mass is directly related to its luminosity, as this luminosity is entirely generated by hydrogen shell burning. As such a star, composed of a small dense core surrounded by an extended convective envelope, is forced to move up the Hayashi track its luminosity increases strongly with only a fairly modest decrease in temperature. Hence one also finds a relationship between the giant’s radius and the mass of its degenerate helium core – almost entirely independent of the mass present in the hydrogen-rich envelope (Refsdal & Weigert 1971; Webbink, Rappaport & Savonije 1983). This relationship is very important for LMXBs and wide-orbit binary

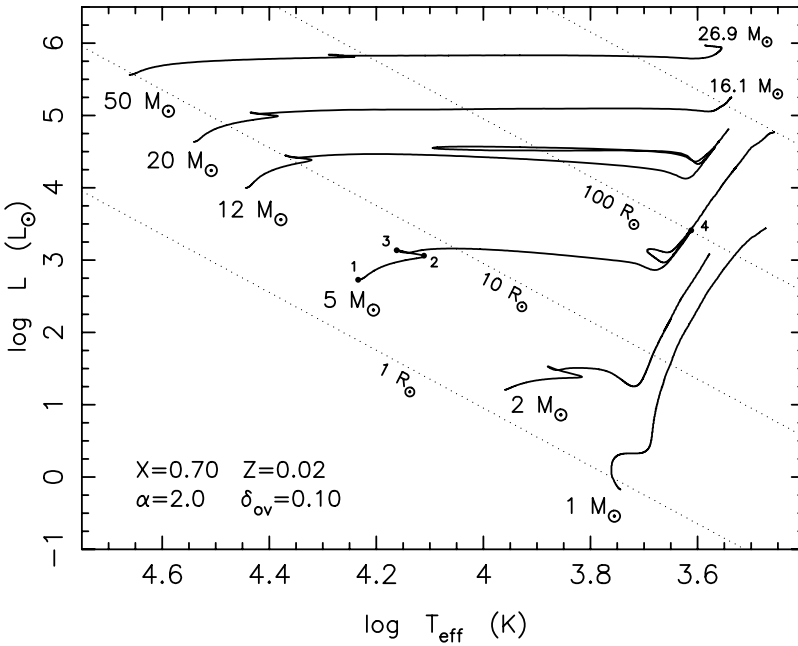


Fig. 16.5. Stellar evolutionary tracks in the H-R diagram.

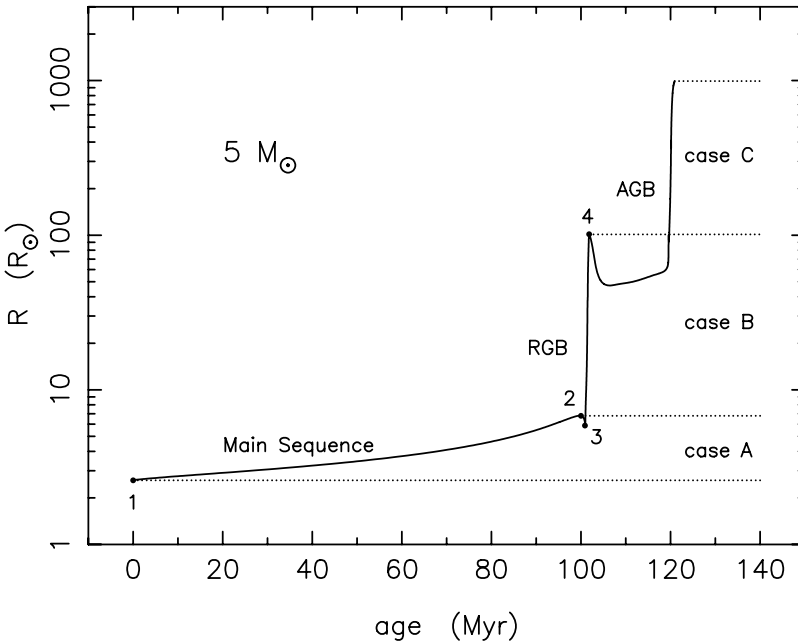


Fig. 16.6. Evolutionary change of the radius of the  $5 M_{\odot}$  star plotted in Fig. 16.5. The ranges of radii for mass transfer to a companion star in a binary system according to RLO cases A, B and C are indicated – see Section 16.4 for an explanation.

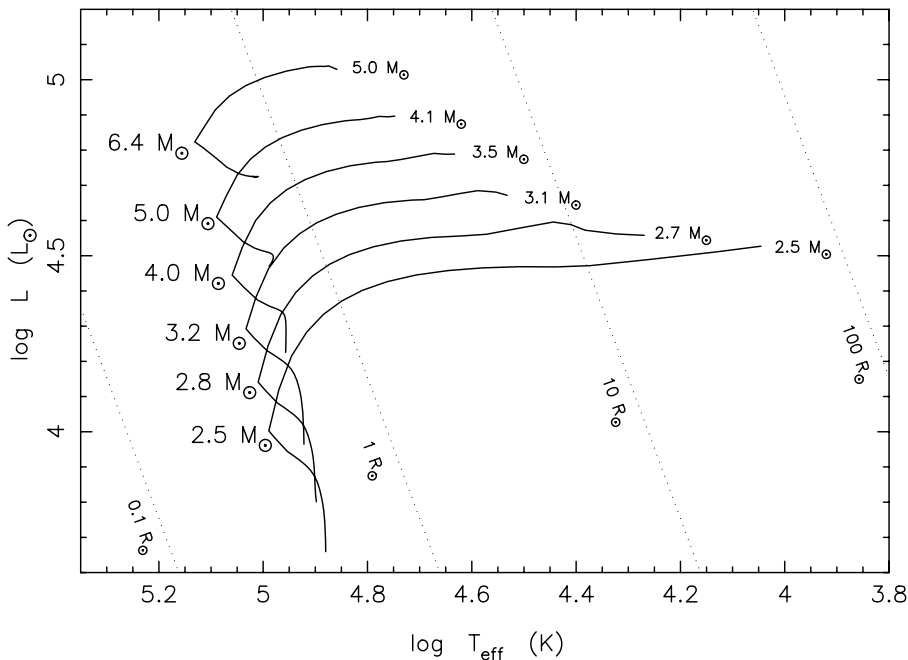


Fig. 16.7. Evolutionary tracks of 2.5–6.4  $M_{\odot}$  helium stars ( $Y = 0.98$ ,  $Z = 0.02$ ). The final stellar mass (after wind mass loss) is written at the end of the tracks. The expansion of low-mass helium stars in close binaries often results in a second mass-transfer phase (case BB RLO). This plot was made with data provided by O. Pols (2002, private communication).

pulsars since, as we shall see later on, it results in a relationship between orbital period and white dwarf mass.

### 16.3.3 The evolution of helium stars

For low-mass stars, the evolution of the helium core in post main-sequence stars is practically independent of the presence of an extended hydrogen-rich envelope. However, for more massive stars ( $> 2.3 M_{\odot}$ ) the evolution of the core of an isolated star differs from that of a naked helium star (i.e., a star that has lost its hydrogen envelope via mass transfer in a close binary system). Thus, it is very important to study the giant phases of helium star evolution. Pioneering studies in this field are those of Paczyński (1971), Nomoto (1984) and Habets (1986). Of particular interest are the low-mass helium stars ( $M_{\text{He}} < 3.5 M_{\odot}$ ) since they swell up to large radii during their late evolution – see Fig. 16.7. This may cause an additional phase of mass transfer from the naked helium star to its companion (often referred to as so-called case BB mass transfer). Recent detailed studies of helium stars in binaries have been performed by Dewi *et al.* (2002). Using helium star models ( $Z = 0.03$ ,  $Y = 0.97$ ) calculated by O. Pols (2002, private communication), we fitted the helium star ZAMS radii as a function of mass:

$$R_{\text{He}} = 0.212(M_{\text{He}}/M_{\odot})^{0.654} R_{\odot} \quad (16.7)$$

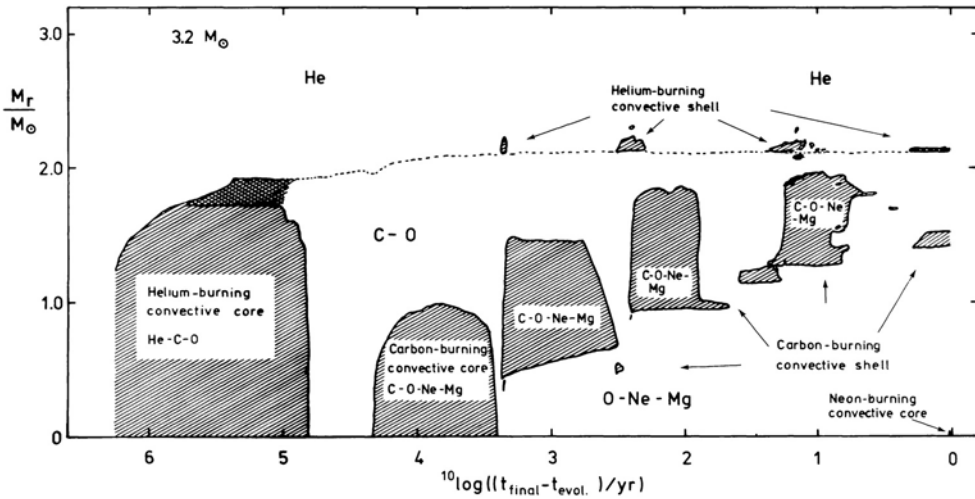


Fig. 16.8. The interior evolution of a  $3.2 M_{\odot}$  helium star. Hatched regions are convective; double hatched regions are semi-convective. The broken line indicates the region of maximum net energy generation in the helium-burning shell (approx. the boundary between the CO core and its adjacent helium layer). After Habets (1986).

It is important to realize that helium cores in binaries have tiny envelopes of hydrogen ( $< 0.01 M_{\odot}$ ) when they detach from RLO. This has important effects on their subsequent radial evolution (e.g., Han *et al.* 2002).

The evolution of more massive helium stars (Wolf–Rayet stars) is also quite important. There is currently no clear agreement on the rate of intense-wind mass loss from Wolf–Rayet stars (e.g., Wellstein & Langer 1999; Nugis & Lamers 2000; Nelemans & van den Heuvel 2001). A best-estimate fit to the wind mass-loss rate of Wolf–Rayet stars is, for example, given by Dewi *et al.* (2002):

$$\dot{M}_{\text{He, wind}} = \begin{cases} 2.8 \times 10^{-13} (L/L_{\odot})^{1.5} M_{\odot} \text{ yr}^{-1}, & \log(L/L_{\odot}) \geq 4.5 \\ 4.0 \times 10^{-37} (L/L_{\odot})^{6.8} M_{\odot} \text{ yr}^{-1}, & \log(L/L_{\odot}) < 4.5 \end{cases} \quad (16.8)$$

The uncertainty in determining this rate also affects our knowledge of the threshold mass for core collapse into a black hole (Schaller *et al.* 1992; Woosley, Langer & Weaver 1995; Brown, Lee & Bethe 1999). Very important in this respect is the question of whether the helium star is “naked” or “embedded” – i.e., is the helium core of the massive star surrounded by a thick hydrogen mantle? In the latter case this helium “star” does not lose much mass in the form of a wind and it can go through all burning stages and terminate as a black hole. Single star evolutionary models suggest that this happens above an initial stellar mass of  $\geq 19 M_{\odot}$ , as around this mass a sudden increase in the mass of the collapsing iron core occurs to  $\geq 1.9 M_{\odot}$  (Woosley & Weaver 1995). In order to form a black hole in a close binary, it is best to keep the helium core embedded in its hydrogen envelope as long as possible, i.e., to start from a wide “case C” binary evolution, as has been convincingly argued by Brown, Lee & Bethe (1999); Wellstein & Langer (1999); Brown *et al.* (2001) and Nelemans & van den Heuvel (2001). In this case, common envelope evolution (Section 16.5) leads to a narrow system consisting of the evolved helium core and the low-mass companion. The helium core collapses to a black hole and produces a supernova in this process, shortly after the spiral-in. When the low-mass

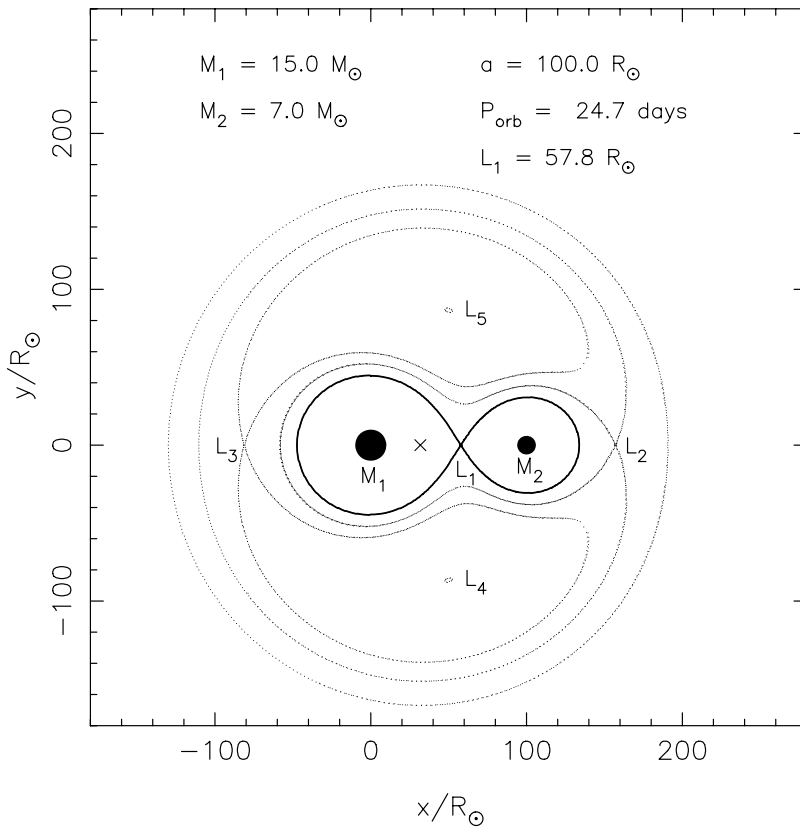


Fig. 16.9. A cross-section in the equatorial plane of the critical equipotential surfaces in a binary. The thick curve crossing through  $L_1$  is the Roche-lobe.

companion evolves to fill its Roche-lobe these systems are observed as soft X-ray transients (SXTs) – see Section 16.2.4.

### 16.4 Roche-lobe overflow: cases A, B and C

The effective gravitational potential in a binary system is determined by the masses of the stars and the centrifugal force arising from the motion of the two stars around one another. One may write this potential as

$$\Phi = -\frac{GM_1}{r_1} - \frac{GM_2}{r_2} - \frac{\Omega^2 r_3^2}{2} \tag{16.9}$$

where  $r_1$  and  $r_2$  are the distances to the center of the stars with mass  $M_1$  and  $M_2$ , respectively;  $\Omega$  is the orbital angular velocity; and  $r_3$  is the distance to the rotational axis of the binary. It is assumed that the stars are small with respect to the distance between them and that they revolve in circular orbits, i.e.,  $\Omega = \sqrt{GM/a^3}$ . In a binary where tidal forces have circularized the orbit, and brought the two stellar components into synchronized co-rotation, one can define fixed equipotential surfaces in a comoving frame (see e.g., van den Heuvel 1994). The equipotential surface passing through the first Lagrangian point,  $L_1$ , defines the

“pear-shaped” Roche-lobe – see the cross-section in Fig. 16.9. If the initially more massive star (the donor) evolves to fill its Roche-lobe the unbalanced pressure at  $L_1$  will initiate mass transfer (Roche-lobe overflow, RLO) onto its companion star (the accretor). The radius of the donor’s Roche-lobe,  $R_L$ , is defined as that of a sphere with the same volume as the lobe. It is a function only of the orbital separation,  $a$ , and the mass ratio,  $q \equiv M_{\text{donor}}/M_{\text{accretor}}$ , of the binary components. It can be approximated as (Eggleton 1983)

$$\frac{R_L}{a} = \frac{0.49 q^{2/3}}{0.6 q^{2/3} + \ln(1 + q^{1/3})} \quad (16.10)$$

A star born in a close binary system with a radius smaller than that of its Roche-lobe may, either because of expansion of its envelope at a later evolutionary stage or because the binary shrinks sufficiently as a result of orbital angular momentum losses, begin RLO. The further evolution of the system will now depend on the evolutionary state and structure of the donor star at the onset of the overflow, which is determined by  $M_{\text{donor}}$  and  $a$ , as well as the nature of the accreting star. Kippenhahn and Weigert (1967) define three types of RLO: cases A, B and C. In case A, the system is so close that the donor star begins to fill its Roche-lobe during core-hydrogen burning; in case B the primary star begins to fill its Roche-lobe after the end of core-hydrogen burning but before helium ignition; in case C it overflows its Roche-lobe during helium shell burning or beyond. It is clear from Fig. 16.6 that cases B and C occur over a wide range of radii (orbital periods); case C even up to orbital periods of  $\sim 10$  years. The precise orbital period ranges for cases A, B and C depend on the initial donor star mass and on the mass ratio. Once the RLO has started it continues until the donor has lost its hydrogen-rich envelope (typically  $\geq 70\%$  of its total mass) and subsequently no longer fills its Roche-lobe.

#### 16.4.1 *The orbital angular momentum balance equation*

The orbital angular momentum of a binary system is given by

$$J_{\text{orb}} = \frac{M_1 M_2}{M} \Omega a^2 \sqrt{1 - e^2} \quad (16.11)$$

where  $a$  is the separation between the stellar components;  $M_1$  and  $M_2$  are the masses of the accretor and donor star, respectively;  $M = M_1 + M_2$  and the orbital angular velocity  $\Omega = \sqrt{GM/a^3}$ . Here  $G$  is the constant of gravity. As mentioned earlier, tidal effects acting on a near-RLO (giant) star will circularize the orbit on a short timescale of  $\sim 10^4$  yr (Verbunt & Phinney 1995). In the following we therefore neglect any small eccentricity ( $e = 0$ ). A simple logarithmic differentiation of the above equation yields the rate of change in orbital separation:

$$\frac{\dot{a}}{a} = 2 \frac{\dot{J}_{\text{orb}}}{J_{\text{orb}}} - 2 \frac{\dot{M}_1}{M_1} - 2 \frac{\dot{M}_2}{M_2} + \frac{\dot{M}_1 + \dot{M}_2}{M} \quad (16.12)$$

where the total change in orbital angular momentum is given by

$$\frac{\dot{J}_{\text{orb}}}{J_{\text{orb}}} = \frac{\dot{J}_{\text{gwr}}}{J_{\text{orb}}} + \frac{\dot{J}_{\text{mb}}}{J_{\text{orb}}} + \frac{\dot{J}_{\text{ls}}}{J_{\text{orb}}} + \frac{\dot{J}_{\text{ml}}}{J_{\text{orb}}} \quad (16.13)$$

These two equations constitute the orbital angular momentum balance equation and will now be discussed in more detail. The first term on the right-hand side of Eq. (16.13) gives the change in orbital angular momentum due to gravitational wave radiation (Landau &

Lifshitz 1958):

$$\frac{J_{\text{gwr}}}{J_{\text{orb}}} = -\frac{32 G^3}{5 c^5} \frac{M_1 M_2 M}{a^4} \text{ s}^{-1} \tag{16.14}$$

where  $c$  is the speed of light in vacuum. The validity of this mechanism has been beautifully demonstrated in PSR 1913+16, which is an ideal GTR-laboratory (e.g., Taylor & Weisberg 1989). For sufficiently narrow orbits the above equation becomes the dominant term in Eq. (16.13) and will cause  $a$  to decrease. Therefore, the orbits of very narrow binaries will tend to shrink continuously, forcing the components into contact. Gravitational radiation losses are a major force driving the mass transfer in very narrow binaries, such as CVs and LMXBs (Faulkner 1971).

The second term in Eq. (16.13) arises due to so-called magnetic braking. The presence of magnetic stellar winds has long been known to decelerate the rotation of low-mass stars (e.g., Kraft 1967; Skumanich 1972; Sonderblom 1983). The loss of spin angular momentum is caused by the magnetic field that exists as a result of chromospheric coronal activity of cool  $\lesssim 1.5 M_{\odot}$  stars with sub-photospheric convection zones (Mestel 1984). In tight synchronized binaries, the loss of spin angular momentum occurs at the expense of the orbital angular momentum. As a result the orbital period decreases while the stellar components spin up, due to tidal forces, and approach one another. Based on Skumanich’s observations, Verbunt and Zwaan (1981) derived an expression for the effect of the magnetic braking and applied it to LMXBs by extrapolating, the dependence of the magnetic braking on the orbital angular velocity, down to very short orbital periods (of the order  $\sim$  hours):

$$\frac{J_{\text{mb}}}{J_{\text{orb}}} \simeq -0.5 \times 10^{-28} f_{\text{mb}}^{-2} \frac{k^2 R_2^4}{a^5} \frac{GM^3}{M_1 M_2} \text{ s}^{-1} \tag{16.15}$$

(in cgs units) where  $R_2$  is the radius of the mass-losing star;  $k^2$  is its gyration radius and  $f_{\text{mb}}$  is a constant of order unity. However, a fundamental law of angular momentum loss is unknown for rapidly rotating stars. Rappaport, Verbunt and Joss (1983) investigated a weaker dependency on the stellar radius. Meanwhile, it now seems that the necessary stellar activity may saturate for rotation periods shorter than  $\sim 2\text{--}3$  days (e.g., Rucinski 1983; Vilhu & Walter 1987), which leads to a much flatter dependence of the angular momentum loss rate on the angular velocity ( $\dot{J}_{\text{mb}} \propto \Omega^{1.2}$ ) than is given by the Skumanich law ( $\dot{J}_{\text{mb}} \propto \Omega^3$ ). Based partly on observational work, Stepien (1995) derived a new magnetic braking law which smoothly matches the Skumanich-law dependence for wide systems to the dependence obtained by Rucinski (1983) for short orbital period ( $\lesssim 3$  days) systems:

$$\frac{J_{\text{mb}}}{J_{\text{orb}}} \simeq -1.90 \times 10^{-16} \frac{k^2 R_2^2}{a^2} \frac{M^2}{M_1 M_2} e^{-1.50 \times 10^{-5} / \Omega} \text{ s}^{-1} \tag{16.16}$$

The two formulas above represent a strong and a weak magnetic braking torque, respectively, and their relative strength can be compared in, e.g., Tauris (2001). For a recent discussion see also Eggleton (2001). It should be noted that for many years it was thought that the magnetic field has to be anchored in underlying radiative layers of a star (Parker 1955). However, recent observations and calculations, e.g., by Dorch and Nordlund (2001), seem to suggest that even fully convective stars still operate a significant magnetic field. This conclusion has important consequences for the explanation of the observed period gap in CVs (Spruit & Ritter 1983). We encourage further investigations on this topic.

The third term ( $\dot{J}_{\text{ls}}/J_{\text{orb}}$ ) on the right-hand side of Eq. (16.13) describes possible exchange of angular momentum between the orbit and the donor star due to its expansion or contraction. Tauris (2001) calculated the pre-RLO spin-orbit couplings in LMXBs and demonstrated that the sole nuclear expansion of a (sub)giant donor in a tight binary will lead to an orbital period *decrease* by  $\sim 10\%$ , prior to the onset of the RLO mass transfer, as a result of tidal interactions. This effect is most efficient for binaries with  $2 < P_{\text{orb}} < 5$  days. In more narrow orbits the donor star does not expand very much and for wide binaries the tidal torque is weak. However, when the effect of magnetic braking is included in the calculations prior to RLO it will dominate the loss of orbital angular momentum if its corresponding torque is relatively strong. The tidal torque in LMXBs can be determined by considering the effect of turbulent viscosity in the convective envelope of the donor on the equilibrium tide (Terquem *et al.* 1998). In very wide orbit LMXBs ( $P_{\text{orb}} > 100$  days) the orbital separation will always *widen* prior to RLO since the stellar wind mass loss becomes very important for such giant stars. To quantize this effect one can apply the Reimers (1975) wind mass-loss rate:

$$\dot{M}_{\text{wind}} = -4 \times 10^{13} \eta_{\text{RW}} L R/M M_{\odot} \text{ yr}^{-1} \quad (16.17)$$

where the luminosity, radius and mass of the mass-losing star are in solar units and  $\eta_{\text{RW}} \simeq 0.5$  is a mass-loss parameter.

Spin-orbit couplings in X-ray binaries can also help to stabilize the mass-transfer processes in IMXBs with radiative donor stars (Tauris & Savonije 2001). In such systems the effect of pumping spin angular momentum into the orbit is clearly seen in the calculations as a result of a contracting mass-losing star in a tidally locked system. This causes the orbit to widen (or shrink less) and survive the, otherwise dynamically unstable, mass transfer.

The tidal effects in eccentric high-mass binary systems are discussed in, e.g., Witte & Savonije (1999) and Witte (2001). For massive donor stars ( $> 8 M_{\odot}$ ) one can use the mass-loss rates by, e.g., de Jager, Nieuwenhuijzen & van der Hucht (1988).

Finally, the last term on the right-hand side of Eq. (16.13) represents the change in orbital angular momentum caused by mass loss from the binary system. This is usually the dominant term in the orbital angular momentum balance equation and its total effect is given by

$$\frac{\dot{J}_{\text{ml}}}{J_{\text{orb}}} = \frac{\alpha + \beta q^2 + \delta \gamma (1 + q)^2}{1 + q} \frac{\dot{M}_2}{M_2} \quad (16.18)$$

where  $\alpha$ ,  $\beta$  and  $\delta$  are the fractions of mass lost from the donor in the form of a direct fast wind, the mass ejected from the vicinity of the accretor and from a circumbinary co-planar toroid (with radius,  $a_r = \gamma^2 a$ ), respectively (see van den Heuvel (1994) and Soberman, Phinney & van den Heuvel (1997)). The accretion efficiency of the accreting star is thus given by  $\epsilon = 1 - \alpha - \beta - \delta$ , or equivalently

$$\partial M_1 = -(1 - \alpha - \beta - \delta) \partial M_2 \quad (16.19)$$

where  $\partial M_2 < 0$  ( $M_2$  refers to the donor star). These factors will be functions of time as the binary system evolves during the mass-transfer phase.

The general solution for calculating the change in orbital separation during the X-ray phase is found by integration of the orbital angular momentum balance equation (Eq. 16.12). It is often a good approximation to assume  $\dot{J}_{\text{gwr}}, \dot{J}_{\text{mb}} \ll \dot{J}_{\text{ml}}$  during short RLO, and if  $\alpha$ ,  $\beta$  and  $\delta$

are constant in time:

$$\frac{a}{a_0} = \Gamma_{\text{ls}} \left( \frac{q}{q_0} \right)^{2(\alpha+\gamma\delta-1)} \left( \frac{q+1}{q_0+1} \right)^{\frac{-\alpha-\beta+\delta}{1-\epsilon}} \left( \frac{\epsilon q+1}{\epsilon q_0+1} \right)^{3+2\frac{\alpha\epsilon^2+\beta+\gamma\delta(1-\epsilon)^2}{\epsilon(1-\epsilon)}} \quad (16.20)$$

where the subscript 0 denotes initial values and  $\Gamma_{\text{ls}}$  is factor of order unity to account for the tidal spin-orbit couplings ( $\dot{J}_{\text{ls}}$ ) other than the magnetic braking ( $\dot{J}_{\text{mb}}$ ). We remind the reader that  $q \equiv M_{\text{donor}}/M_{\text{accretor}}$ .

### 16.4.2 Stability criteria for mass transfer

The stability and nature of the mass transfer is very important in binary stellar evolution. It depends on the response of the mass-losing donor star and of the Roche-lobe – see Soberman, Phinney & van den Heuvel (1997) for a review. If the mass transfer proceeds on a short timescale (thermal or dynamical) the system is unlikely to be observed during this short phase; whereas if the the mass transfer proceeds on a nuclear timescale it is still able to sustain a high enough accretion rate onto the neutron star or black hole for the system to be observed as an X-ray source for a long time.

When the donor star fills its Roche-lobe, and is perturbed by removal of mass, it falls out of hydrostatic and thermal equilibrium. In the process of re-establishing equilibrium the star will either grow or shrink – first on a dynamical (sound crossing) timescale, and then on a slower thermal (Kelvin–Helmholtz) timescale. But also the Roche-lobe changes in response to the mass transfer/loss. As long as the donor star’s Roche-lobe continues to enclose the star the mass transfer is stable. Otherwise it is unstable and proceeds on a dynamical timescale. Hence the question of stability is determined by a comparison of the exponents in power-law fits of radius to mass,  $R \sim M^\zeta$ , for the donor star and the Roche-lobe respectively:

$$\zeta_{\text{donor}} \equiv \frac{\partial \ln R_2}{\partial \ln M_2} \quad \wedge \quad \zeta_{\text{L}} \equiv \frac{\partial \ln R_{\text{L}}}{\partial \ln M_2} \quad (16.21)$$

where  $R_2$  and  $M_2$  refer to the mass-losing donor star. Given  $R_2 = R_{\text{L}}$  (the condition at the onset of RLO) the initial stability criteria becomes

$$\zeta_{\text{L}} \leq \zeta_{\text{donor}} \quad (16.22)$$

where  $\zeta_{\text{donor}}$  is the adiabatic or thermal (or somewhere in between) response of the donor star to mass loss. Note that the stability might change during the mass-transfer phase so that initially stable systems become unstable, or vice versa, later in the evolution (e.g., Kalogera & Webbink 1996). The radius of the donor is a function of time and mass and thus

$$\dot{R}_2 = \left. \frac{\partial R_2}{\partial t} \right|_{M_2} + R_2 \zeta_{\text{donor}} \frac{\dot{M}_2}{M_2} \quad (16.23)$$

$$\dot{R}_{\text{L}} = \left. \frac{\partial R_{\text{L}}}{\partial t} \right|_{M_2} + R_{\text{L}} \zeta_{\text{L}} \frac{\dot{M}_2}{M_2} \quad (16.24)$$

The second terms on the right-hand sides follow from Eq. (16.21); the first term of Eq. (16.23) is due to expansion of the donor star as a result of nuclear burning (e.g., shell hydrogen burning on the RGB) and the first term in Eq. (16.24) represents changes in  $R_{\text{L}}$  that are not caused by mass transfer – such as orbital decay due to gravitational wave radiation and tidal spin-orbit couplings. Tidal couplings act to synchronize the orbit whenever the rotation of the donor is perturbed (e.g., as a result of magnetic braking or an increase in the moment of inertia while

the donor expands). The mass-loss rate of the donor can be found as a self-consistent solution to Eqs. (16.23) and (16.24) assuming  $\dot{R}_2 = \dot{R}_L$  for stable mass transfer.

**16.4.3 Response of the Roche-lobe to mass transfer/loss**

In order to study the dynamical evolution of an X-ray binary let us consider the cases where tidal interactions and gravitational wave radiation can be neglected. We shall also assume that the amount of mass lost directly from the donor star in the form of a fast wind, or via a circumbinary toroid, is negligible compared to the flow of material transferred via the Roche-lobe. Hence we have  $J_{\text{gwr}} = J_{\text{mb}} = J_{\text{ls}} = 0$  and  $J_{\text{ml}}/J_{\text{orb}} = \beta q^2/(1 + q) \times (\dot{M}_2/M_2)$ . This corresponds to the mode of “isotropic re-emission” where matter flows over from the donor star onto the compact accretor (neutron star or black hole) in a conservative way, before a fraction,  $\beta$ , of this material is ejected isotropically from the system with the specific angular momentum of the accretor, i.e.,  $\dot{M}_1 = -(1 - \beta)\dot{M}_2$ ,  $dJ_{\text{orb}} = (J_1/M_1)\beta dM_2$  and  $J_1 = (M_2/M) J_{\text{orb}}$ . In the above formalism this corresponds to  $\alpha = \delta = 0$  and  $\Gamma_{\text{ls}} = 1$ . This is actually a good approximation for many real systems (with orbital periods longer than a few days). Following Tauris and Savonije (1999) one can then combine Eqs. (16.10), (16.19) and (16.20) and obtain an analytical expression for  $\zeta_L$ :

$$\begin{aligned} \zeta_L &= \frac{\partial \ln R_L}{\partial \ln M_2} = \left( \frac{\partial \ln a}{\partial \ln q} + \frac{\partial \ln(R_L/a)}{\partial \ln q} \right) \frac{\partial \ln q}{\partial \ln M_2} \\ &= [1 + (1 - \beta)q]\psi + (5 - 3\beta)q \end{aligned} \tag{16.25}$$

where

$$\psi = \left[ -\frac{4}{3} - \frac{q}{1 + q} - \frac{2/5 + 1/3 q^{-1/3}(1 + q^{1/3})^{-1}}{0.6 + q^{-2/3} \ln(1 + q^{1/3})} \right] \tag{16.26}$$

In the limiting case where  $q \rightarrow 0$  (when the accretor is much heavier than the donor star; for example in a soft X-ray transient system hosting a black hole):

$$\lim_{q \rightarrow 0} \zeta_L = -5/3 \tag{16.27}$$

The behavior of  $\zeta_L(q, \beta)$  for different X-ray binaries is plotted in Fig. 16.10. This figure is quite useful to get an idea of the stability of the mass transfer when comparing with  $\zeta$  of the donor star. We see that in general the Roche-lobe,  $R_L$ , increases ( $\zeta_L < 0$ ) when material is transferred from a relatively light donor to a heavy accretor ( $q < 0$ ). In this situation the mass transfer will be stable. Correspondingly  $R_L$  decreases ( $\zeta_L > 0$ ) when material is transferred from a heavy donor to a lighter accretor ( $q > 0$ ). In this case the mass transfer has the potential to be dynamically unstable. This behavior can be understood from the bottom panel of Fig. 16.10 where we plot

$$-\partial \ln(a)/\partial \ln(q) = 2 + \frac{q}{q + 1} + q \frac{3\beta - 5}{q(1 - \beta) + 1} \tag{16.28}$$

as a function of  $q$ . The sign of this quantity is important since it tells whether the orbit expands or contracts in response to mass transfer (note  $\partial q < 0$ ). It is noticed that the orbit always expands when  $q < 1$  and it always decreases when  $q > 1.28$  (solving  $\partial \ln(a)/\partial \ln(q) = 0$  for  $\beta = 1$  yields  $q = (1 + \sqrt{17})/4 \approx 1.28$ ). If  $\beta > 0$  the orbit can still expand for  $1 < q < 1.28$ . There is a point at  $q = 3/2$  where  $\partial \ln(a)/\partial \ln(q) = 2/5$ , independent of  $\beta$ . It should also be mentioned for the curious reader that if  $\beta > 0$  then, in some cases, it is actually possible for a binary to decrease its separation,  $a$ , while increasing  $P_{\text{orb}}$  at the same time!

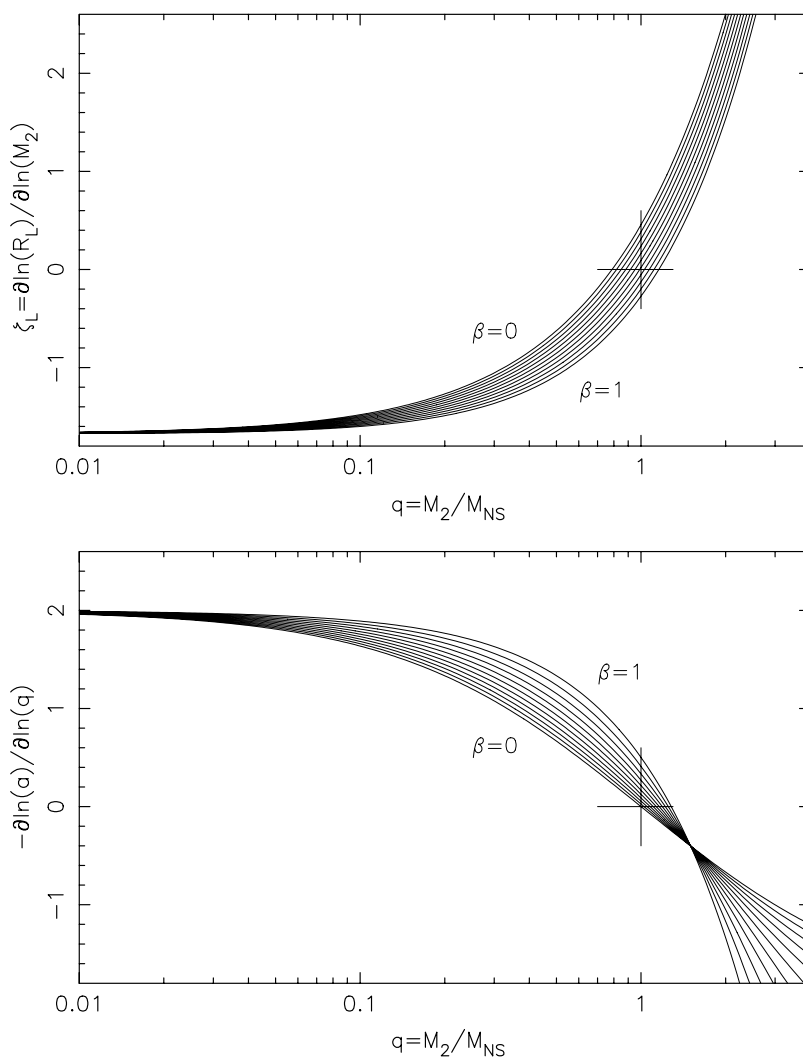


Fig. 16.10. Top panel: the Roche-radius exponent ( $R_L \propto M_2^{\zeta_L}$ ) for LMXBs as a function of  $q$  and  $\beta$ . The different curves correspond to different constant values of  $\beta$  in steps of 0.1. Tidal effects are not taken into account and the mass loss is according to the isotropic re-emission model (i.e.,  $\alpha = 0$ ,  $\delta = 0$ ). A cross is shown to highlight the cases of  $q = 1$  and  $\zeta_L = 0$ . In the bottom panel we have plotted  $-\partial \ln a / \partial \ln q$  as a function of  $q$ . When this quantity is positive the orbit widens. This is the case when  $q \leq 1$ . For more massive donor stars ( $q > 1$ ) the orbit shrinks in response to mass transfer. Since  $M_2$  (and hence  $q$ ) is decreasing with time the evolution during the mass-transfer phase follows these curves from right to left, although  $\beta$  need not be constant. After Tauris & Savonije (1999).

#### 16.4.4 Response of the mass-losing star: the effect on the binary

The radius of the mass-losing donor star will respond to mass loss. Therefore, in order to obtain a full stability analysis of the mass-transfer process it is important to know whether or not the donor star expands (or contracts) in response to mass loss. This is determined by the stellar structure (i.e., temperature gradient and entropy) of the envelope at the onset of the RLO.

*16.4.4.1 Donor stars with a radiative envelope*

Donor stars with radiative (or only slightly convective) envelopes will usually shrink (or keep a roughly constant radius) in response to mass loss. Therefore, these stars will give rise to a dynamically stable mass-transfer phase if the mass ratio,  $q$  is not too large. Calculations by Tauris and Savonije (1999) show that all LMXBs with donor stars  $M_2 \leq 1.8 M_\odot$  and a neutron star will have a stable mass-transfer phase. Podsiadlowski, Rappaport and Pfahl (2002) find an upper limit for stability of  $2.0 M_\odot$ . Stars with radiative envelopes are not very evolved and hence they are only found as donor stars in systems with short orbital periods ( $P_{\text{orb}} \lesssim 20$  days) at the onset of the RLO. Recently it was demonstrated in detail that even IMXB systems with radiative donor stars  $2 < M_2/M_\odot < 5$  are able to survive extreme mass transfer on a sub-thermal timescale (Tauris, van den Heuvel & Savonije 2000).

*16.4.4.2 Donor stars with a convective envelope*

The thermal response of a donor star with a deep convective envelope is much more radical. It expands rapidly in response to mass loss due to the super-adiabatic temperature gradient in its giant envelope. This is clearly an unstable situation if the Roche-lobe does not grow accordingly. For systems with  $q \gtrsim 1.5$  (heavy donors) the orbital shrinking is so efficient that, in combination with an expanding convective donor, it always leads to the formation of a common envelope and (dynamically unstable) spiral-in evolution. Hence, this is most likely the destiny for all HMXBs.

**16.5 Common envelope evolution**

A very important stage of the evolution of close binaries is the formation of a common envelope (CE). This phase is accompanied by the creation of a drag force, arising from the motion of the companion star through the envelope of the evolved star, which leads to dissipation of orbital angular momentum (spiral-in process) and deposition of orbital energy in the envelope. Hence, the global outcome of a CE-phase is reduction of the binary separation and often ejection of the envelope. There is strong evidence of orbital shrinkage (as brought about by frictional torques in a CE-phase) in some observed close binary pulsars and white dwarf binaries, e.g., PSR 1913+16, PSR J1756–5322 and L 870–2. In these systems it is clear that the precursor of the last-formed degenerate star must have achieved a radius much larger than the current orbital separation. There are many uncertainties involved in calculations of the spiral-in phase during the CE evolution. The evolution is often tidally unstable and the angular momentum transfer, dissipation of orbital energy and structural changes of the donor star take place on very short timescales ( $\sim 10^3$  yr). A complete study of the problem requires very detailed multi-dimensional hydrodynamical calculations. For a general review on common envelopes, see, e.g., Iben & Livio (1993) and Taam & Sandquist (2000).

A simple estimation of the reduction of the orbital separation can be found by equating the binding energy of the envelope of the (sub)giant donor to the required difference in orbital energy (before and after the CE-phase). Following the formalism of Webbink (1984) and de Kool (1990), let  $0 < \eta_{\text{CE}} < 1$  describe the efficiency of ejecting the envelope, i.e., of converting orbital energy into the kinetic energy that provides the outward motion of the envelope:  $E_{\text{env}} \equiv \eta_{\text{CE}} \Delta E_{\text{orb}}$  or,

$$\frac{GM_{\text{donor}}M_{\text{env}}}{\lambda a_i r_L} \equiv \eta_{\text{CE}} \left[ \frac{GM_{\text{core}}M_1}{2a_f} - \frac{GM_{\text{donor}}M_1}{2a_i} \right] \quad (16.29)$$

yielding the ratio of final (post-CE) to initial (pre-CE) orbital separation:

$$\frac{a_f}{a_i} = \frac{M_{\text{core}} M_1}{M_{\text{donor}}} \frac{1}{M_1 + 2M_{\text{env}}/(\eta_{\text{CE}} \lambda r_L)} \quad (16.30)$$

where  $M_{\text{core}} = M_{\text{donor}} - M_{\text{env}}$ ;  $r_L = R_L/a_i$  is the dimensionless Roche-lobe radius of the donor star so that  $a_i r_L = R_L \approx R_{\text{donor}}$  and  $\lambda$  is a parameter that depends on the stellar mass–density distribution, and consequently also on the evolutionary stage of the star. The orbital separation of the surviving binaries is quite often reduced by a factor of  $\sim 100$  as a result of the spiral-in. If there is not enough orbital energy available to eject the envelope the stellar components will merge in this process.

### 16.5.1 The binding energy of the envelope

The total binding energy of the envelope to the core is given by

$$E_{\text{bind}} = - \int_{M_{\text{core}}}^{M_{\text{donor}}} \frac{GM(r)}{r} dm + \alpha_{\text{th}} \int_{M_{\text{core}}}^{M_{\text{donor}}} U dm \quad (16.31)$$

where the first term is the gravitational binding energy and  $U$  is the internal thermodynamic energy. The latter involves the basic thermal energy for a simple perfect gas ( $3\mathfrak{N}T/2\mu$ ), the energy of radiation ( $aT^4/3\rho$ ), as well as terms due to ionization of atoms and dissociation of molecules and the Fermi energy of a degenerate electron gas (Han *et al.* 1994, 1995). The value of  $\alpha_{\text{th}}$  depends on the details of the ejection process, which are very uncertain. A value of  $\alpha_{\text{th}}$  equal to 0 or 1 corresponds to maximum and minimum envelope binding energy, respectively. By simply equating Eqs. (16.29) and (16.31) one is able to calculate the parameter  $\lambda$  for different evolutionary stages of a given star.

Dewi and Tauris (2000) and Tauris and Dewi (2001) were the first to publish detailed calculations on the binding energy of the envelope to determine the  $\lambda$ -parameter (however, see also Bisscheroux 1999). Dewi and Tauris (2000) investigated stars with masses  $3 - 10 M_{\odot}$  and found that while  $\lambda < 1$  on the RGB,  $\lambda \gg 1$  on the AGB (especially for stars with  $M < 6 M_{\odot}$ ). Hence, the envelopes of these donor stars on the AGB are easily ejected; with only a relatively modest decrease in orbital separation resulting from the spiral-in. For more massive stars ( $M > 10 M_{\odot}$ )  $\lambda < 0.1 - 0.01$  (see Fig. 16.11) and the internal energy is not very dominant (Dewi & Tauris 2001; Podsiadlowski, Rappaport & Han 2003). This result has the important consequence that many HMXBs will not produce double neutron star systems because they coalesce during their subsequent CE-phase (leading to a relatively small merging rate of double neutron star systems, as shown by Voss & Tauris 2003).

It should be noticed that the exact determination of  $\lambda$  depends on how the core boundary is defined (see Tauris & Dewi 2001 for a discussion). For example, if the core boundary (bifurcation point of envelope ejection in a CE) of the  $20 M_{\odot}$  star in Fig. 16.11 is moved out by  $0.1 M_{\odot}$  then  $\lambda$  is typically increased by a factor of  $\sim 2$ .

#### 16.5.1.1 The question of hyper-critical accretion onto a NS in a CE

It has been argued that a neutron star spiralling inwards in a common envelope might experience hyper-critical accretion and thereby collapse into a black hole (e.g., Chevalier 1993; Brown 1995; Bethe & Brown 1998; Fryer, Woosley & Hartmann 1999). However, this idea seems difficult to reconcile with the observations of a number of very tight-orbit binary pulsars. For example, the systems PSR J1756–5322 and PSR B0655+64, which have

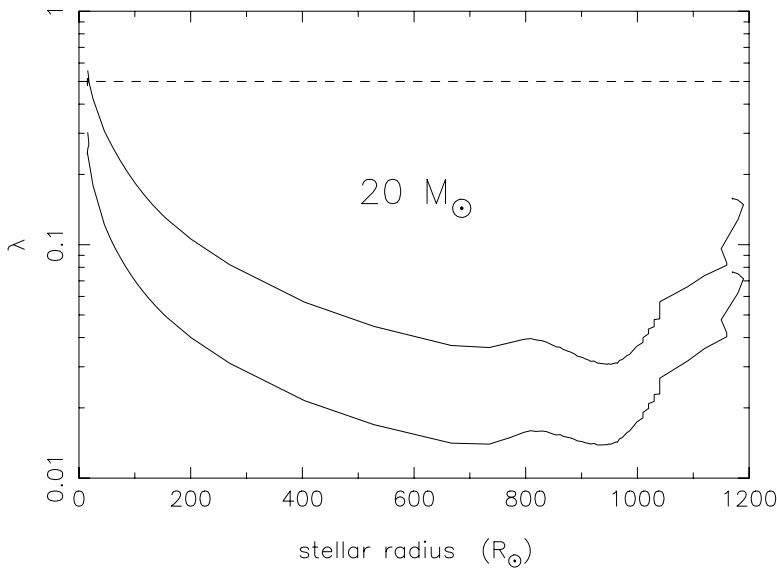


Fig. 16.11. The  $\lambda$ -parameter for a  $20 M_{\odot}$  star as a function of stellar radius. The upper curve includes internal thermodynamic energy ( $\alpha_{\text{th}} = 1$ ) whereas the lower curve is based on the sole gravitational binding energy ( $\alpha_{\text{th}} = 0$ ) – see Eq. (16.31). There is a factor  $\sim 2$  in difference between the  $\lambda$ -curves in accordance with the virial theorem. It is a common misconception to use a constant value of  $\lambda = 0.5$  (marked by the dashed line). See text for details.

massive CO white dwarf companions ( $\sim 0.7 M_{\odot}$  and  $\sim 1 M_{\odot}$ ) with orbital periods of only 0.45 and 1.06 days, respectively. From an evolutionary point of view there is no other way to produce such systems apart from a CE and spiral-in phase with donor masses between  $3 M_{\odot}$  and  $6 M_{\odot}$ . From a theoretical point of view it has been argued that the hyper-critical accretion can be inhibited by rotation (Chevalier 1996) and strong outflows from the accretion disk (Armitage & Livio 2000). Finally, it should be noticed that the masses of neutron stars determined in all of the five detected Galactic double neutron star systems are quite similar and close to a value of  $1.4 M_{\odot}$ . Hence, in all these cases it is clear that the first-born neutron star did not accrete any significant amount of material from the common envelope.

## 16.6 (Asymmetric) supernova explosions in close binaries

After a close binary star has lost its H-envelope, and possibly also its He-envelope, during RLO and/or CE evolution it will collapse and explode in a supernova (SN) if it is massive enough. The critical threshold mass for a helium star to form a neutron star is about  $2.8 M_{\odot}$  (and somewhat lower for a CO-star, i.e., a helium star that has lost its helium envelope via case BB RLO). This value corresponds roughly to an initial mass of  $10 M_{\odot}$  ( $\sim 10 M_{\odot}$  for case C, and  $\sim 12 M_{\odot}$  for case B/A RLO). If the core mass is below this critical threshold mass the star contracts, possibly after a second phase of RLO, and settles peacefully as a cooling white dwarf. If  $M_{\text{He}} \gtrsim 8 M_{\odot}$  the supernova leaves behind a black hole. All observed neutron stars in binary pulsars seem to have been born with a canonical mass of  $1.3 - 1.4 M_{\odot}$ . Neutron stars in LMXBs may afterwards possibly accrete up to  $\sim 1 M_{\odot}$  before collapsing

further into a black hole (see Section 16.7.3). In very massive X-ray binaries, neutron stars can probably be born with higher masses  $\sim 1.8 M_{\odot}$  (Barziv *et al.* 2001).

As mentioned in the introduction, there is firm evidence that most newborn neutron stars receive a momentum kick at birth which gives rise to the high velocities observed (typically  $\sim 400 \text{ km s}^{-1}$ ), although there also may well be a smaller fraction  $\sim 10\text{--}20\%$  that receive kicks  $\lesssim 50 \text{ km s}^{-1}$  in order to explain the observed neutron stars in globular clusters and the population of very wide-orbit X-ray binaries (Pfahl *et al.* 2002). It is still an open question whether or not black holes also receive a kick at birth. At least in some cases there are observational indications of mass ejection during their formation, as in any successful supernova explosion (Iwamoto *et al.* 1998), and the recent determination of the runaway velocity ( $112 \pm 18 \text{ km s}^{-1}$ ) of the black hole binary GRO J1655–40 (Mirabel *et al.* 2002) also seems to suggest that the formation of black holes is accompanied by a kick.

In an excellent paper Hills (1983) calculated the dynamical consequences of binaries surviving an asymmetric SN. Tauris and Takens (1998) generalized the problem and derived analytical formulas for the velocities of stellar components ejected from disrupted binaries and also included the effect of shell impact on the companion star. If the collapsing core of a helium star results in a supernova explosion it is a good approximation that the collapse is instantaneous compared with  $P_{\text{orb}}$ . Here we summarize a few important equations. The orbital energy of a binary is given by

$$E_{\text{orb}} = -\frac{GM_1M_2}{2a} = -\frac{GM_1M_2}{r} + \frac{1}{2}\mu v_{\text{rel}}^2 \tag{16.32}$$

where  $r$  is the separation between the stars at the moment of explosion;  $\mu$  is the reduced mass of the system and  $v_{\text{rel}} = \sqrt{GM/r}$  is the relative velocity of the two stars in a circular pre-SN binary. The change of the semi-major axis as a result of the SN is then given by (Flannery & van den Heuvel 1975)

$$\frac{a}{a_0} = \left[ \frac{1 - (\Delta M/M)}{1 - 2(\Delta M/M) - (w/v_{\text{rel}})^2 - 2 \cos \theta (w/v_{\text{rel}})} \right] \tag{16.33}$$

where  $a_0 = r$  and  $a$  are the initial and final semi-major axis, respectively;  $\Delta M$  is the amount of matter lost in the SN;  $w$  is the magnitude of the kick velocity and  $\theta$  is the direction of the kick relative to the orientation of the pre-SN velocity. The orientation of the kick magnitude is probably completely uncorrelated with respect to the orientation of the binary – the escaping neutrinos from deep inside the collapsing core are not aware that they are members of a binary system (see, however, Pfahl *et al.* (2002) and Dewi, Podsiadlowski & Pols (2005) for the hypothesis that the kick *magnitude* may depend on the pre-SN history of the collapsing core). For each binary and a sufficiently high value of  $w$  there exists a critical angle,  $\theta_{\text{crit}}$ , for which a SN with  $\theta < \theta_{\text{crit}}$  will result in disruption of the orbit (i.e., if the denominator of Eq. (16.33) is less than zero).

The sudden mass loss in the SN affects the bound orbit with an eccentricity

$$e = \sqrt{1 + \frac{2E_{\text{orb}}L_{\text{orb}}^2}{\mu G^2 M_1^2 M_2^2}} \tag{16.34}$$

where the orbital angular momentum can be derived from (see also Eq. (16.11))

$$L_{\text{orb}} = |\mathbf{r} \times \mathbf{p}| = r\mu\sqrt{(v_{\text{rel}} + w \cos \theta)^2 + (w \sin \theta \sin \phi)^2} \tag{16.35}$$

Note, in the two equations above  $v_{\text{rel}}$  is the pre-SN relative velocity of the two stars, whereas the stellar masses and  $\mu$  now refer to the post-SN values.

Systems surviving the SN will receive a recoil velocity from the combined effect of instant mass loss and a kick. One can easily find this velocity,  $v_{\text{sys}}$ , from conservation of momentum. Let us consider a star with mass  $M_{\text{core}}$  collapsing to form a neutron star with mass  $M_{\text{NS}}$  and hence

$$v_{\text{sys}} = \sqrt{\Delta P_x^2 + \Delta P_y^2 + \Delta P_z^2} / (M_{\text{NS}} + M_2) \quad (16.36)$$

where the change in momentum is

$$\begin{aligned} \Delta P_x &= M_{\text{NS}}(v_{\text{core}} + w \cos \theta) - M_{\text{core}}v_{\text{core}} \\ \Delta P_y &= M_{\text{NS}}w \sin \theta \cos \phi \\ \Delta P_z &= M_{\text{NS}}w \sin \theta \sin \phi \end{aligned} \quad (16.37)$$

and where  $M_2$  is the unchanged mass of the companion star;  $v_{\text{core}}$  is the pre-SN velocity of the collapsing core, in a center of mass reference frame, and  $\phi$  is the angle between the projection of  $\mathbf{w}$  onto a plane  $\perp$  to  $\mathbf{v}_{\text{core}}$  (i.e.,  $w_y = w \sin \theta \cos \phi$ ). Beware, if the post-SN periastron distance,  $a(1 - e)$ , is smaller than the radius of the companion star then the binary will merge.

It is important to realize the difference between *gravitational* mass (as measured by an observer) and *baryonic* mass of a neutron star. The latter is  $\sim 15\%$  larger for a typical equation-of-state. When considering dynamical effects on binaries surviving a SN this fact is often (almost always) ignored!

## 16.7 Evolution of LMXBs: formation of millisecond pulsars

Figure 16.12 depicts the formation of an LMXB and millisecond pulsar system. There are now more than 40 binary millisecond pulsars (BMSPs) known in the Galactic disk. They can be roughly divided into three observational classes (Tauris 1996): class A contains the wide-orbit ( $P_{\text{orb}} > 20$  days) BMSPs with low-mass helium white dwarf companions ( $M_{\text{WD}} < 0.45 M_{\odot}$ ), whereas the close-orbit BMSPs ( $P_{\text{orb}} \lesssim 15$  days) consist of systems with either low-mass helium white dwarf companions (class B) or systems with relatively heavy CO/O-Ne-Mg white dwarf companions (class C). The last class evolved through a phase with significant loss of angular momentum (either common envelope evolution or extreme mass transfer on a sub-thermal timescale) and descends from IMXBs with donors:  $2 < M_2/M_{\odot} < 8$ , see Fig. 16.13. The single MSPs are believed to originate from tight class B systems where the companion has been destroyed or evaporated – either from X-ray irradiation when the neutron star was accreting, or in the form of a pulsar radiation/wind of relativistic particles (e.g., van den Heuvel & van Paradijs 1988; Ruderman, Shaham & Tavani 1989; Ergma & Fedorova 1991; Podsiadlowski 1991; Shaham 1992; Tavani 1992). Observational evidence for this scenario is found in eclipsing MSPs with ultra-light companions – e.g., PSR 1957+20 ( $P_{\text{orb}} = 0.38$  days;  $M_2 \simeq 0.02 M_{\odot}$ ) and the planetary pulsar PSR 1257+12 (Wolszczan 1994).

For LMXBs it has been shown by Pylyser and Savonije (1988, 1989) that an orbital bifurcation period separates the formation of converging systems (which evolve with decreasing  $P_{\text{orb}}$  until the mass-losing component becomes degenerate and an ultra-compact binary is formed) from the diverging systems (which finally evolve with increasing  $P_{\text{orb}}$  until the

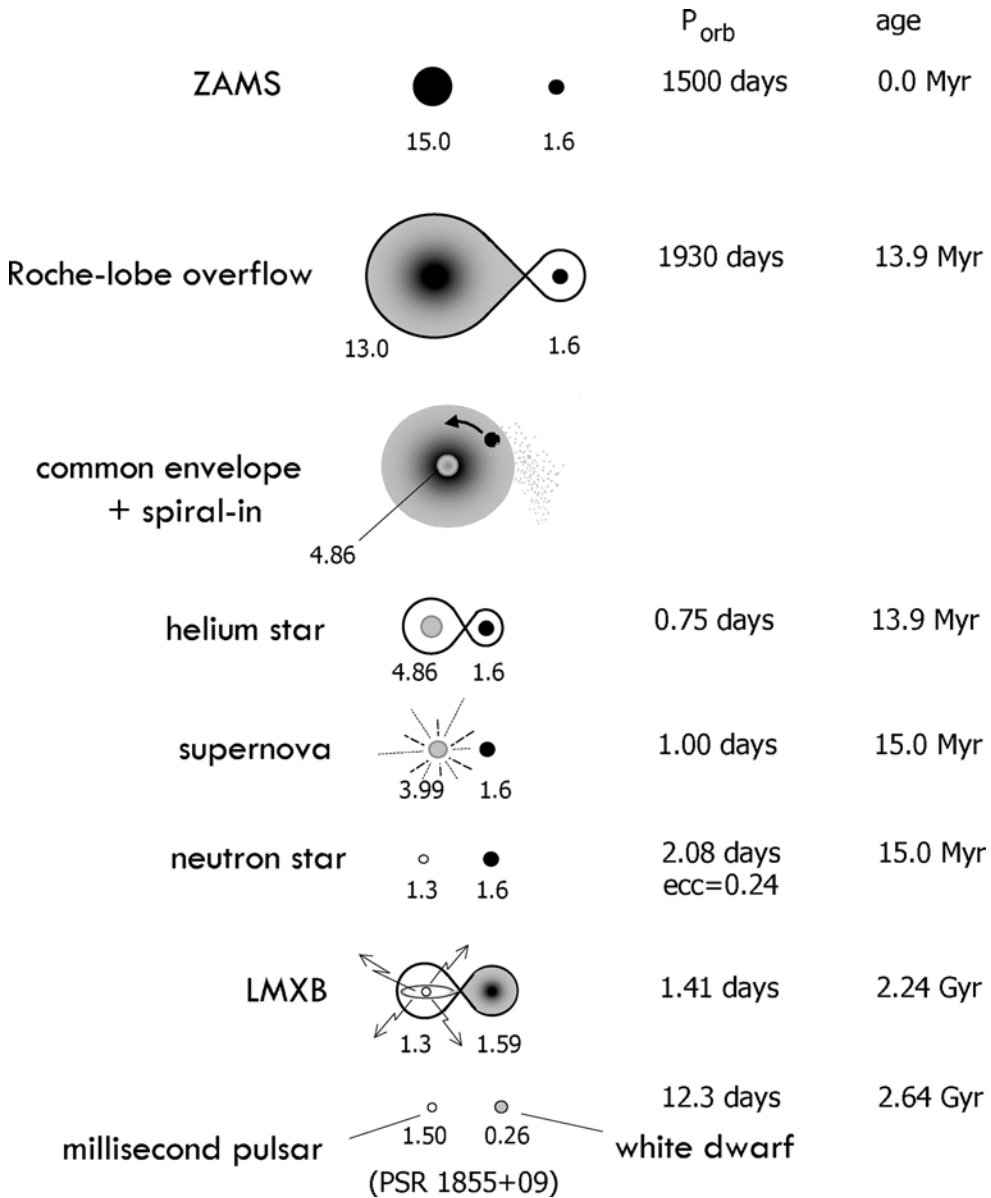


Fig. 16.12. Cartoon depicting the evolution of a binary system eventually leading to an LMXB and finally the formation of a binary millisecond pulsar. Parameters governing the specific orbital angular momentum of ejected matter, the common envelope and spiral-in phase, the asymmetric supernova explosion and the stellar evolution of the naked helium star all have a large impact on the exact evolution. Parameters are given for a scenario leading to the formation of the observed binary millisecond pulsar PSR 1855+09. The stellar masses given are in solar units.

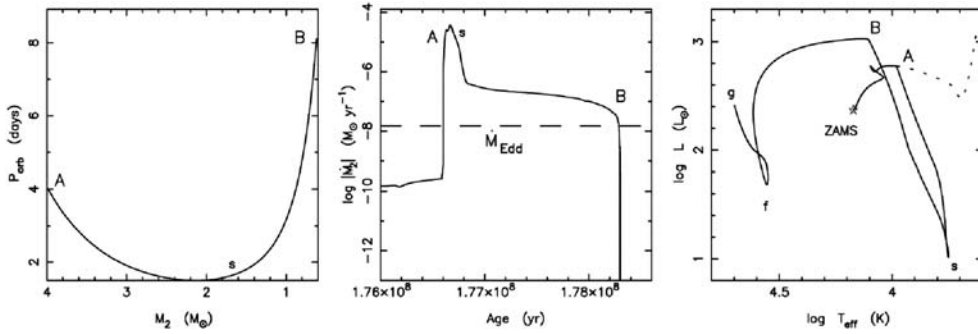


Fig. 16.13. The evolution of an IMXB leading to the formation of a BMSP with a CO WD companion in a close orbit. The initial configuration was a  $4 M_{\odot}$  donor star and a neutron star with an orbital period of 4 days. The mass-transfer phase is between points A and B. Between points f and g helium is burning in the core of the stripped companion star. After Tauris, van den Heuvel & Savonije (2000).

mass-losing star has lost its envelope and a wide detached binary is formed). This important bifurcation period is about 2–3 days depending on the strength of the magnetic braking torque.

**16.7.1 Formation of wide-orbit binary millisecond pulsars**

In LMXBs with initial  $P_{\text{orb}} > 2$  days the mass transfer is driven by internal thermonuclear evolution of the donor star since it evolves into a (sub)giant before loss of orbital angular momentum dominates. These systems have been studied by Webbink, Rappaport and Savonije (1983), Taam (1983), Savonije (1987), Joss, Rappaport and Lewis (1987), Rappaport *et al.* (1995) and more recently Ergma, Sarna and Antipova (1998), Tauris and Savonije (1999) and Podsiadlowski, Rappaport and Pfahl (2002). For a donor star on the red giant branch (RGB) the growth in core mass is directly related to the luminosity, as this luminosity is entirely generated by hydrogen shell burning. As such a star, with a small compact core surrounded by an extended convective envelope, is forced to move up the Hayashi track its luminosity increases strongly with only a fairly modest decrease in temperature. Hence one also finds a relationship between the giant’s radius and the mass of its degenerate helium core – almost entirely independent of the mass present in the hydrogen-rich envelope (see Table 16.5). It has also been argued that the core mass determines the rate of mass transfer (Webbink, Rappaport & Savonije 1983). In the scenario under consideration, the extended envelope of the giant is expected to fill its Roche-lobe until termination of the mass transfer. Since the Roche-lobe radius,  $R_L$ , only depends on the masses and separation between the two stars, it is clear that the core mass, from the moment the star begins RLO, is uniquely correlated with  $P_{\text{orb}}$  of the system. Thus the final orbital period ( $\sim 2$  to  $10^3$  days) is expected to be a function of the mass of the resulting white dwarf companion (Savonije 1987). Tauris and Savonije (1999) calculated the expected  $(P_{\text{orb}}, M_{\text{WD}})$  correlation in detail and found an overall best fit:

$$M_{\text{WD}} = \left( \frac{P_{\text{orb}}}{b} \right)^{1/a} + c \tag{16.38}$$

Table 16.5. Stellar parameters for giant stars with  $R = 50.0 R_{\odot}$

$M_{\text{initial}}/M_{\odot}$	1.0*	1.6*	1.0**	1.6**
$\log L/L_{\odot}$	2.644	2.723	2.566	2.624
$\log T_{\text{eff}}$	3.573	3.593	3.554	3.569
$M_{\text{core}}/M_{\odot}$	0.342	0.354	0.336	0.345
$M_{\text{env}}/M_{\odot}$	0.615	1.217	0.215	0.514

\* Single star ( $X = 0.70$ ,  $Z = 0.02$  and  $\alpha = 2.0$ ,  $\delta_{\text{ov}} = 0.10$ ).

\*\* Binary star (at onset of RLO:  $P_{\text{orb}} \simeq 60$  days and  $M_{\text{NS}} = 1.3 M_{\odot}$ ). After Tauris & Savonije (1999).

where, depending on the chemical composition of the donor,

$$(a, b, c) = \begin{cases} 4.50 & 1.2 \times 10^5 & 0.120 & \text{Pop. I} \\ 4.75 & 1.1 \times 10^5 & 0.115 & \text{Pop. I+II} \\ 5.00 & 1.0 \times 10^5 & 0.110 & \text{Pop. II} \end{cases} \quad (16.39)$$

Here  $M_{\text{WD}}$  is in solar mass units and  $P_{\text{orb}}$  is measured in days. The fit is valid for BMSPs with helium white dwarf companions and  $0.18 \leq M_{\text{WD}}/M_{\odot} \leq 0.45$ . The formula depends slightly on the adopted value of the convective mixing-length parameter. It should be noted that the correlation is *independent* of  $\beta$  (the fraction of the transferred material lost from the system – see Section 16.4.1), the mode of the mass loss and the strength of the magnetic braking torque, since the relation between giant radius and core mass of the donor star remains unaffected by the exterior stellar conditions governing the process of mass transfer. However, for the *individual* binary  $P_{\text{orb}}$  and  $M_{\text{WD}}$  do depend on these parameters. In Fig. 16.14 we have plotted a theoretical ( $P_{\text{orb}}$ ,  $M_{\text{WD}}$ ) correlation and also plotted evolutionary tracks calculated for four LMXBs. Although clearly the class of BMSPs with helium white dwarf companions is present, the estimated masses of the BMSP white dwarfs are quite uncertain, since they depend on the unknown orbital inclination angle and the pulsar mass, and no clear observed ( $P_{\text{orb}}$ ,  $M_{\text{WD}}$ ) correlation has yet been established from the current observations. In particular there may be a discrepancy for the BMSPs with  $P_{\text{orb}} \gtrsim 100$  days (Tauris 1996).

### 16.7.2 Formation of close-orbit binary millisecond pulsars

In LMXBs with initial  $P_{\text{orb}} < 2$  days the mass transfer is driven by loss of angular momentum due to magnetic braking and gravitational wave radiation. The evolution of such systems is very similar to the evolution of CVs – see e.g. Spruit & Ritter (1983); Verbunt & van den Heuvel (1995); Ergma, Sarna & Antipova (1998) and Chapter 10 by Kuulkers *et al.*

### 16.7.3 Masses of binary neutron stars

In general, the masses of binary pulsars can only be estimated from their observed mass function, which depends on the unknown orbital inclination angle. Only in a few tight systems is it possible to directly measure post-Newtonian parameters (e.g., the general relativistic Shapiro delay) which yield precise values of the stellar masses (see Taylor & Weisberg 1989). For example, in the double neutron star system PSR 1913+16 the (gravitational) masses are known to be 1.441 and 1.387  $M_{\odot}$ . Although the majority of the (rough)

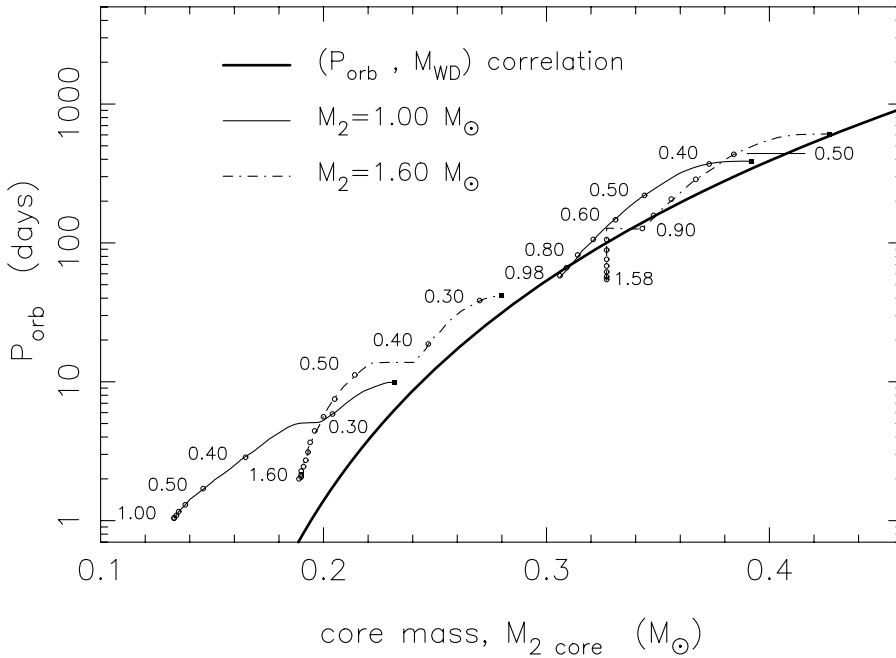


Fig. 16.14. Evolutionary tracks of four LMXBs showing  $P_{\text{orb}}$  as a function of  $M_{\text{core}}$  of the donor star. The initial donor masses were 1.0 and  $1.6 M_{\odot}$  (each calculated at two different initial  $P_{\text{orb}}$ ) and the initial neutron star mass was  $1.3 M_{\odot}$ . The total mass of the donors during the evolution is written along the tracks. At the termination of the mass-transfer process the donor only has a tiny ( $\leq 0.01 M_{\odot}$ ) H-envelope and the end-points of the evolutionary tracks are located near the curve representing the  $(P_{\text{orb}}, M_{\text{WD}})$  correlation for BMSPs. After Tauris & Savonije (1999).

estimated pulsar masses may be consistent with the canonical value of  $\sim 1.4 M_{\odot}$  (Thorsett & Chakrabarty 1999), one could still expect a spread in neutron star masses from an evolutionary point of view. The recycled pulsars in double neutron star systems, for example, did not have a chance to accrete much material because of the short-lived common envelope and spiral-in phase that these systems evolved through, according to the standard model. Assuming all neutron stars to be born with a mass of  $1.3 M_{\odot}$ , Tauris and Savonije (1999) demonstrated that an  $(P_{\text{orb}}, M_{\text{NS}})$  anti-correlation would be expected for millisecond pulsars as a simple consequence of the interplay between mass-transfer rate (and thus accretion rate), orbital period and the evolutionary status of the LMXB donor star at the onset of the RLO. However, since this model predicted rather massive ( $> 2 M_{\odot}$ ) neutron stars in binary millisecond pulsar systems with  $P_{\text{orb}} \lesssim 30$  days, it failed to explain the mass of PSR B1855+09 ( $P_{\text{orb}} = 12.3$  days), which is known to be  $< 1.55 M_{\odot}$  from constraints on its Shapiro delay. The authors concluded that this was a proof for the fact that a large amount of matter *must* be lost from the LMXB even for sub-Eddington accretion – probably as a result of either accretion disk instabilities (Pringle 1981; van Paradijs 1996) or the so-called propeller effect (Illarionov & Sunyaev 1985).

The maximum mass of a neutron star depends on the equation of state for dense matter. Barziv *et al.* (2001) reported that the HMXB Vela X-1 has a neutron star mass  $\sim 1.86 M_{\odot}$ . Furthermore, some kHz QPO sources are claimed to host heavy ( $> 2 M_{\odot}$ ) neutron stars. If

this is the case, then all soft EOS, including some kaon condensation EOS (Brown & Bethe 1994; Bethe & Brown 1995), can be ruled out.

## 16.8 Evolution of HMXBs

### 16.8.1 Formation of double neutron star/black hole binaries

The formation of a HMXB requires two relatively massive stars ( $> 12 M_{\odot}$ ). Alternatively the secondary ZAMS star can be less massive initially, as long as it gains sufficient material from the primary star to later end up above the threshold mass for undergoing a supernova explosion (like the primary star). The first mass-transfer phase, from the primary to the secondary star, is usually assumed to be dynamically stable (semi-conservative) if the mass ratio at the onset of the RLO is not too extreme. However, later on *all* HMXBs end up in a common envelope phase, as the neutron star (or low-mass black hole) is engulfed by the extended envelope of its companion, in an orbit that is rapidly shrinking due to heavy loss of orbital angular momentum. As discussed earlier in Section 16.3.3, stellar winds of massive stars, as well as naked helium cores (Wolf-Rayet stars), are some of the most uncertain aspects of the modeling of HMXB evolution. The physical conditions that determine the formation of a neutron star versus a black hole are also still quite unknown. It may well be that core mass is not the only important factor to determine the outcome. Magnetic field and spin of the collapsing core could also play a major role (Ergma & van den Heuvel 1998). Furthermore, it seems clear from observations that there is an overlap in the mass range for making a neutron star versus a black hole.

### 16.8.2 Gravitational waves and merging NS/BH binaries

The rate of energy loss as a result of gravitational wave radiation (GWR) is given by (in the quadrupole approximation,  $a \ll \lambda_{\text{gwr}}$ )

$$L_{\text{gwr}} = \left| \frac{dE}{dt} \right| = \frac{G}{5c^5} \langle \ddot{Q}_{jk} \ddot{Q}_{jk} \rangle g(n, e) \simeq \frac{32G^4}{5c^5} \frac{M^3 \mu^2}{a^5} f(e) \quad (16.40)$$

where  $Q$  denotes the quadrupole moment of the mass distribution;  $M$  is the total mass of the system;  $\mu$  is the reduced mass and  $f(e)$  is a function of the orbital eccentricity (here we have disregarded the dependence on the harmonic number of the wave signal). The energy loss due to GWR can only be subtracted from the orbital energy of the binary and hence the orbital separation will decrease as

$$\dot{a} = \frac{GM\mu}{2E_{\text{orb}}^2} \dot{E}_{\text{orb}} \quad \left( a = -\frac{GM\mu}{2E_{\text{orb}}} \wedge \dot{E}_{\text{orb}} = -L_{\text{gwr}} \right) \quad (16.41)$$

For an eccentric binary:

$$\frac{1}{a} \frac{da}{dt} = -\frac{1}{E} \left. \frac{dE}{dt} \right|_{e=0} f(e) \quad \wedge \quad f(e) \simeq \frac{1 + \frac{73}{24}e^2 + \frac{37}{96}e^4}{(1 - e^2)^{7/2}} \quad (16.42)$$

where the approximate fit for  $f(e)$  above is given by Peters (1964).

Now we have an expression for the rate of change in the orbital separation:

$$\dot{a} \simeq -\frac{64G^3}{5c^5} \frac{M^2 \mu}{a^3} \frac{1 + \frac{73}{24}e^2 + \frac{37}{96}e^4}{(1 - e^2)^{7/2}} \quad (16.43)$$

which can be transformed into an expression for the merging time,  $\tau_{\text{gwr}}$  (Peters 1964) as a

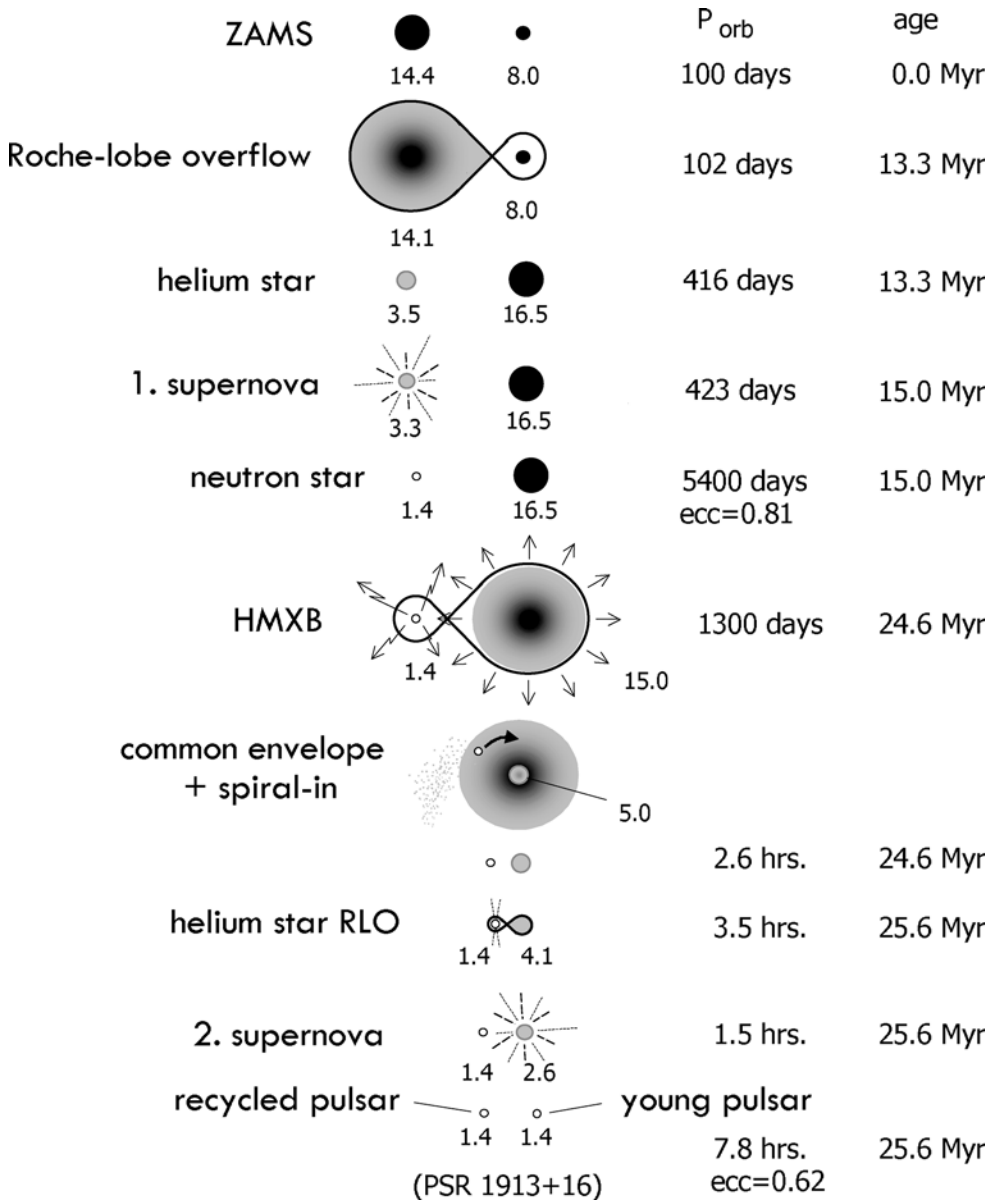


Fig. 16.15. Cartoon depicting the formation of a Be-star/HMXB and finally a double neutron star system. Such a binary will experience two supernova explosions. In a double pulsar system the recycled pulsar is most likely to be observed as a result of its very long spin-down timescale compared to the young pulsar (a factor of  $\sim 10^2$ ). Tight NS-NS systems will coalesce due to gravitational wave radiation. These collisions should be detected by advanced gravitational wave detectors such as LIGO II/VIRGO.

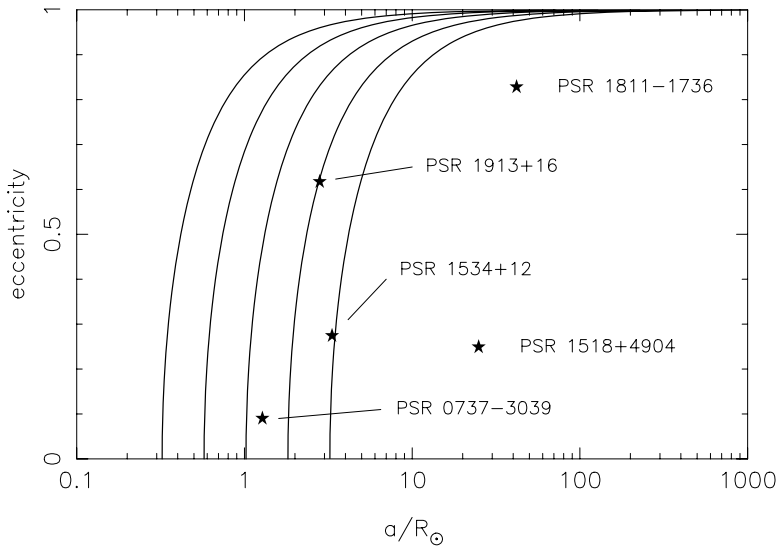


Fig. 16.16. Isochrones for the merging time of double neutron star binaries, as calculated by the authors. The curves correspond to values of (from left to right):  $3 \times 10^5$  yr, 3 Myr, 30 Myr, 300 Myr and 3 Gyr, respectively. The five detected Galactic double neutron star systems are indicated with  $\star$ .

function of the initial values ( $a_0, e_0$ ):

$$\tau_{\text{gwr}}(a_0, e_0) = \frac{12 C_0^4}{19 \beta} \times \int_0^{e_0} \frac{e^{29/19} [1 + (121/304)e^2]^{1181/2299}}{(1 - e^2)^{3/2}} de \tag{16.44}$$

where

$$C_0 = \frac{a_0 (1 - e_0^2)}{e_0^{12/19}} [1 + (121/304)e_0^2]^{-870/2299} \wedge \beta = \frac{64G^3}{5c^5} M^2 \mu \tag{16.45}$$

This equation cannot be solved analytically and must be evaluated numerically. The timescale is very dependent on both  $a$  and  $e$ . Tight and/or eccentric orbits spiral-in much faster than wider and more circular orbits – see Fig. 16.16. For example, we find that the double neutron star system PSR 1913+16 ( $P_{\text{orb}} = 7.75$  hr,  $M_{\text{NS}} = 1.441$  and  $1.387 M_{\odot}$ ) with an eccentricity of 0.617 will merge in 302 Myr; if its orbit was circular the merger time would be five times longer: 1.65 Gyr! For circular orbits the merging timescale can easily be found analytically:  $\tau_{\text{gwr}}^{\text{circ}} = a_0^4/4\beta$ .

### 16.8.2.1 LISA/LIGO observations of signals from tight NS/BH binaries

The recently discovered double pulsar binary system PSR J0737–3039 (Burgay *et al.* 2003) will play a remarkable role for LISA. It has an orbital period  $\sim 2.4$  hr and a distance to the Earth of  $\sim 0.5$  kpc. Continuous emission of gravitational waves should be detected at a strain of  $h \approx 5 \times 10^{-21}$  at a frequency of  $f \approx 0.23$  mHz. Within one year of integration the signal-to-noise ratio is expected to be  $\sim 10$ . Thus this unique system will become an important LISA calibration source. In comparison, the signals from PSR B1913+16 ( $P_{\text{orb}} = 7.75$  hr and  $d \sim 7$  kpc) are too weak, and the wave frequency too small, to be detected by LISA.

However, it is clear from population synthesis studies that many Galactic NS–NS binaries must exist within the detection range of LISA.

The amplitude (or strain) of gravitational waves emitted continuously from a tight binary is given by the sum of the two polarizations of the signal:

$$h = \sqrt{\frac{1}{2} [h_{+, \max}^2 + h_{\times, \max}^2]} = \sqrt{\frac{16\pi G}{c^3} \frac{L_{\text{gwr}}}{\omega_{\text{gwr}} 4\pi d^2}}$$

$$\simeq 1 \times 10^{-21} \left( \frac{M_{\text{chirp}}}{M_{\odot}} \right)^{5/3} \left( \frac{P_{\text{orb}}}{1 \text{ hr}} \right)^{-2/3} \left( \frac{d}{1 \text{ kpc}} \right)^{-1} \quad (16.46)$$

Here the waves are assumed to be sinusoidal with angular frequency,  $\omega_{\text{gwr}}$ , which is  $\sim 2$  times the orbital angular frequency of the binary ( $\Omega = 2\pi/P_{\text{orb}}$ ), and  $M_{\text{chirp}} \equiv \mu^{3/5} M^{2/5}$  is the so-called chirp mass of the system.

As a compact binary continues its inspiral, the gravitational waves will sweep upward in frequency from about 10 Hz to  $10^3$  Hz, at which point the compact stars will collide and coalesce. It is this last 15 minutes of inspiral, with  $\sim 16\,000$  cycles of waveform oscillation, and the final coalescence, that LIGO/VIRGO seeks to monitor. LIGO I and LIGO II are expected to detect NS–NS inspiral events out to a distance of  $\sim 20$  Mpc and  $\sim 300$  Mpc, respectively, according to estimates (Thorne 2001). This corresponds to wave amplitudes of roughly  $10^{-20} > h > 10^{-22}$ . As a result of the much larger chirp mass for the BH–BH mergers, such binaries will be detected out to a distance luminosity,  $d_L \propto M_{\text{chirp}}^{5/6}$  (Finn 1998), which is about 4 times larger. Hence, the ratio of detected event rates for BH–BH mergers relative to NS–NS mergers is  $4^3 \sim 64$  times larger than the corresponding ratio of such mergers in our Galaxy. As a result BH–BH mergers are expected to be dominant for LIGO detectors as noted by Sipior and Sigurdsson (2002).

The cosmological implications of gravitational wave observations of binary inspiral are also interesting to note (Schutz 1986; Finn 1997). Finally, it should be mentioned that LIGO II is expected to detect burst signals from extra-Galactic supernova explosions as well (Thorne 2001). Investigations of these signals may help to reveal the unknown progenitors of both short and long-duration gamma-ray bursts (GRBs).

#### 16.8.2.2 Galactic merger rates of NS/BH binaries

It is very important to constrain the local merging rate of NS/BH-binaries in order to predict the number of events detected by LIGO. This rate can be determined either from binary population synthesis calculations, or from observations of Galactic NS–NS systems (binary pulsars). Both methods involve a large number of uncertainties (e.g., Kalogera *et al.* 2001 and references therein). Therefore, the current estimates for the Galactic merger rate of NS–NS systems cover a wide range:  $10^{-6} - 10^{-3} \text{ yr}^{-1}$ .

The discovery of the very tight binary pulsar system PSR J0737–3039 indicates that the galactic NS–NS merger rate is almost an order of magnitude larger than previously estimated (Burgay *et al.* 2003; Kalogera *et al.* 2004). In addition, the discovery that in this system both neutron stars are observed as radio pulsars, one recycled and one not-recycled (Lyne *et al.* 2004), has provided a beautiful confirmation of the evolutionary model for the formation of double neutron stars depicted in Fig. 16.15 (Srinivasan & van den Heuvel 1982; Lyne *et al.* 2004; van den Heuvel, 2003, 2004).

In order to extrapolate the Galactic coalescence rate out to the volume of the Universe accessible to LIGO, one can either use a method based on star formation rates or a scaling based on the B-band luminosities of galaxies. Using the latter method Kalogera *et al.* (2001) found a scaling factor of  $(1.0 - 1.5) \times 10^{-2} \text{ Mpc}^{-3}$ , or equivalently,  $\sim 400$  for LIGO I (out to 20 Mpc for NS–NS mergers). Since LIGO II is expected to look out to a distance of 300 Mpc (for NS–NS mergers), the volume covered by LIGO II is larger by a factor of  $(300/20)^3$  and thus the scaling factor in this case, relative to the coalescence rates in the Milky Way, is about  $1.3 \times 10^6$ . Therefore, the expected rate of detections from NS–NS inspiral events is roughly between 2 and 500  $\text{yr}^{-1}$  for LIGO II. However, LIGO I may not detect any NS/BH inspiral event.

Recent studies (Voss & Tauris 2003; Dewi, Pols & van den Heuvel 2005) have included “real  $\lambda$ -values” for the CE-phase and this results in a relatively low Galactic NS–NS merger rate (since fewer systems survive the CE evolution). However, Voss and Tauris (2003) also investigated BH–BH systems and find a relatively high Galactic merger rate of such systems, compared to NS–NS systems and mixed NS/BH systems, and estimate a BH–BH merging detection rate of 840  $\text{yr}^{-1}$  for LIGO II.

One should be aware that compact mergers in globular clusters probably also contribute significantly to the total merger rates (Portegies-Zwart & McMillan 2000).

### 16.9 Spin and B-field evolution of accreting neutron stars

Most X-ray pulsars have spin periods between 10 and 1000 s. In persistent sources, spin periods of the order of seconds are found only in systems where we have clear evidence for the presence of an accretion disk from UV and optical observations. These are systems where (a large part of) the mass transfer is due to RLO: the LMXBs and those few HMXBs in which the supergiant donors are just beginning to overflow their Roche-lobes (Cen X-3, SMC X-1 and LMC X-4). The latter are expected to be powered by a combination of stellar wind and beginning atmospheric RLO (Savonije 1978, 1983). In most of these systems the X-ray pulsars show a secular decrease of their pulse period (spin-up) on a relatively short timescale ( $10^3 - 10^5$  yr). Although on short timescales episodes of spin-up and spin-down alternate, the average trend is clearly that of spin-up (see, e.g., Bildsten *et al.* 1997). In sources that are purely wind-fed, the HMXBs with blue supergiant companions that do not yet fill their Roche-lobe, the pulse periods are very long, and they vary erratically in time showing no clear secular trends. This can be explained by the fact that the amount of angular momentum carried by the supersonic winds is negligible, and eddies form in the wind downstream of the neutron star, which alternately may feed co- and counter-rotating angular momentum to it (Taam & Fryxell 1988; Fryxell & Taam 1988; Matsuda *et al.* 1992).

The accretion and spin-evolution of a neutron star in a binary system depend on a number of parameters: the magnetodipole radiation pressure, the ram pressure of the companion star wind, the radius of gravitational capture, the location of the light cylinder, the Alfvén radius, the co-rotation radius, the propeller effect and whether or not an accretion disk is formed – see, e.g., Ghosh & Lamb (1979) and Chapter 13 by King for a detailed description. The old binary neutron stars, which have been spun-up and recycled in LMXBs, reappear as observable millisecond X-ray and radio pulsars. Their so-called equilibrium spin period is given by (see the spin-up line in the  $(P, \dot{P})$ -diagram in Fig. 16.3)

$$P_{\text{eq}} \propto \dot{M}_{\text{NS}}^{-3/7} B^{6/7} R_{\text{NS}}^{18/7} M_{\text{NS}}^{-5/7} \quad (16.47)$$

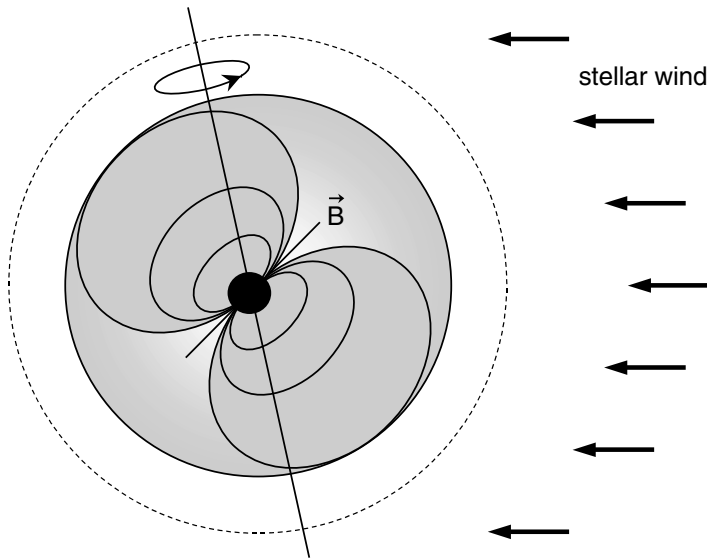


Fig. 16.17. Illustration of the magnetosphere surrounding a wind-accreting neutron star. The rotation period, the magnetic field strength and the ram pressure of the wind determine whether or not accretion onto the neutron star surface is possible. The spin axis and the magnetic field axis are misaligned (thus: a pulsar). X-rays are emitted along the magnetic field axis as the pulsar accretes near its magnetic poles.

As long as  $P > P_{\text{eq}}$  accretion onto the neutron star is possible. Note that, while ordinary single pulsars have a typical lifetime of 10 – 100 Myr, the recycled millisecond pulsars have lifetimes of several Gyr and thus continue to light the sky with beamed pulses for a Hubble-time. The reason for this is simply their low values of  $\dot{P}$ , i.e., relatively weak braking (or radiation-reaction) torques.

### 16.9.1 The Eddington accretion limit

The typical X-ray luminosities of the LMXBs and HMXBs are in the range  $10^{35} - 10^{38} \text{ erg s}^{-1}$ , corresponding to mass accretion rates onto a neutron star in the range  $10^{-11} - 10^{-8} M_{\odot} \text{ yr}^{-1}$ . When the mass-transfer rate exceeds  $\dot{M}_{\text{Edd}} \simeq 1.5 \times 10^{-8} M_{\odot} \text{ yr}^{-1}$  (for spherical accretion of a hydrogen-rich gas), the X-ray luminosity exceeds the so-called Eddington limit at which the radiation pressure force on the accreting matter exceeds the gravitational attraction force of the compact star (Davidson & Ostriker 1973). The concept of an Eddington accretion limit also applies to black holes. At accretion rates  $> \dot{M}_{\text{Edd}}$  the excess accreting matter will pile up around the compact object and form a cloud optically thick to X-rays, thus quenching the source. Therefore, in the observed “persistent” LMXBs and HMXBs the accretion rates must be in the range  $10^{-11} - 10^{-8} M_{\odot} \text{ yr}^{-1}$ . However, the *mass-transfer rate* from the companion star towards the neutron star may be considerably larger. Calculations show that mass transfer exceeding  $10^{-4} M_{\odot} \text{ yr}^{-1}$  may still be dynamically stable (see Fig. 16.13). In cases where super-Eddington mass transfer occurs, the excess material is ejected in a jet – e.g., as observed in the source SS433 (Chapter 9 and King & Begelman 1999).

### 16.9.2 Accretion-induced magnetic field decay

In the past decade it has been possible – under certain assumptions – to compute the accretion-induced magnetic field decay of a binary neutron star – see, e.g., Geppert & Urpin (1994), Konar & Bhattacharya (1997) and Cumming, Zweibel & Bildsten (2001). It is often assumed that the magnetic field has been generated in the outer crust by some unspecified mechanism, e.g., by thermo-magnetic effects (Blandford, Applegate & Hernquist 1983), during or shortly after the neutron star formation. The electrical conductivity in the neutron star crust is mainly a function of mass-density, temperature and degree of lattice impurities. By combining the conductive properties with a cooling model, as well as a temperature profile, one can calculate the evolution of the magnetic field by solving the induction equation:

$$\frac{\partial \mathbf{B}}{\partial t} = -\frac{c^2}{4\pi} \nabla \times \left( \frac{1}{\sigma_{\text{el}}} \times \nabla \times \mathbf{B} \right) + \nabla \times (\mathbf{v} \times \mathbf{B}) \quad (16.48)$$

where  $\mathbf{v}$  is the velocity of accreted material movement and  $\sigma_{\text{el}}$  is the electrical conductivity of the medium. By choosing a simple vector potential, and introducing the so-called Stokes' stream function, the above equation reduces to a second-order partial differential equation, which can be solved numerically. The current distribution, which is responsible for the  $B$ -field, migrates inward as a result of diffusion and enters the highly conducting parts of the neutron star. In that inner region the electrical conductivity is very high (superconducting) and hence the magnetic field will essentially be stable forever – it freezes out at a residual value. The calculated effect of the ohmic dissipation results in final  $B$ -fields of  $\sim 10^8 - 10^9$  G corresponding to the values estimated from observed millisecond pulsars. A very different model, in which it is assumed that the field is anchored in the superconducting and superfluid neutron star core, was put forward by Ruderman (1998) and collaborators. In this physically very elegant model, the field is driven out of the core by rotational slow-down, and also final fields of  $\sim 10^8 - 10^9$  G result. See also the reviews by Bhattacharya & Srinivasan (1995) and Bhattacharya (2002) for further details and alternative models.

In the case of crustal field decay models the next important step would be to solve the evolution self-consistently. That is, to use good stellar evolution models to calculate the mass-transfer rate of the donor star, determine the orbital dynamical response, check whether the material is accreted onto the neutron star or not, determine the crustal temperature from the nuclear burning of accreted material, recalculate the electrical conductivity and its effect on the  $B$ -field. The latter then affects the Alfvén radius, and thus the accretion rate and spin period, which again influences the orbital evolution and response of the donor star, etc. However, our state of understanding of the magnetic field decay mechanisms, and of mass and angular momentum loss mechanisms during binary evolution, is still too fragmentary to allow for a detailed quantitative calculation of the evolution of a rotating magnetized neutron star in a binary system.

### Acknowledgements

TMT gratefully acknowledges support from the Danish Natural Science Research Council under grant no. 56916.

### References

- Alpar, M. A., Cheng, A. F., Ruderman, M. A. and Shaham, J. (1982). *Nature* **300**, 728  
 Armitage, P. J. and Livio, M. (2000). *ApJ* **532**, 540

- Backer, D. C., Kulkarni, S. R., Heiles, C., *et al.* (1982). *Nature* **300**, 615
- Barziv *et al.* (2001). *A&A* **377**, 925
- Beer, M. E. and Podsiadlowski, P. (2002). *MNRAS* **331**, 351
- Bethe, H. A. and Brown, G. E. (1995). *ApJ* **445**, L129  
(1998). *ApJ* **506**, 780
- Bildsten, L., Chakrabarty, D., Chiu, J., *et al.* (1997). *ApJS* **113**, 367
- Bisnovatyi-Kogan, G. S. and Komberg, B. V. (1974). *Astron. Zh.* **51**, 373
- Bisscheroux, B. (1999). Master's thesis, University of Amsterdam (1999)
- Bhattacharya, D. (2002). *JA&A* **23**, 67
- Bhattacharya, D. and van den Heuvel, E. P. J. (1991). *Phys. Rep.* **203**, 1
- Bhattacharya, D. and Srinivasan, G. (1995), in *X-ray Binaries*, eds. W. H. G. Lewin, J. van Paradijs and E. P. J. van den Heuvel (Cambridge University Press)
- Blaauw, A. (1961). *Bull. Astron. Inst. Neth.* **15**, 265
- Blandford, R. D., Applegate, J. H. and Hernquist, L. (1983). *MNRAS* **204**, 1025
- Bolton, C. T. (1972). *Nature* **235**, 271
- Brown, G. E. (1995). *ApJ* **440**, 270
- Brown, G. E. and Bethe, H. A. (1994). *ApJ* **423**, 659
- Brown, G. E., Lee, C. H. and Bethe, H. A. (1999). *New Astronomy* **4**, 313
- Brown, G. E., Heger, A., Langer, N., *et al.* (2001). *New Astronomy* **6**, 457
- Burgay, M., D'Amico, N., Possenti, A., *et al.* (2003). *Nature* **426**, 531
- Chevalier, R. A. (1993). *ApJ* **411**, L33  
(1996). *ApJ* **459**, 322
- Cox, J. P. and Giuli, R.T. (1968). *Stellar Structure, vols. I and II* (New York, Gordon and Breach)
- Cumming, A., Zweibel, E. and Bildsten, L. (2001). *ApJ* **557**, 958
- Davidson, K. and Ostriker, J. P. (1973). *ApJ* **179**, 585
- de Jager, C., Nieuwenhuijzen, H. and van der Hucht, K. A. (1988). *A&AS* **72**, 259
- de Kool, M. (1990). *ApJ* **358**, 189
- Dewey, R. J. and Cordes, J. M. (1987). *ApJ* **321**, 780
- Dewi, J. D. M. and Tauris, T. M. (2000). *A&A* **360**, 1043  
(2001), in *Evolution of Binary and Multiple Star Systems*, eds. P. Podsiadlowski *et al.* (ASP Conf. Vol. 229) p. 255
- Dewi, J. D. M., Pols, O. R., Savonije, G. J. and van den Heuvel, E. P. J. (2002). *MNRAS* **331**, 1027
- Dewi, J. D. M., Podsiadlowski, P. and Pols, O. R. (2005). *MNRAS* **363**, L71
- Dewi, J. D. M., Pols, O. R. and van den Heuvel, E. P. J. (2005). *MNRAS*, submitted
- Dorch, S. B. F. and Nordlund, Å. (2001). *A&A* **365**, 562
- Eggleton, P. P. (1983). *ApJ* **268**, 368  
(2001), in *Evolution of Binary and Multiple Star Systems*, eds. P. Podsiadlowski *et al.* (ASP Conf. Vol. 229)
- Ergma, E. and Fedorova, A. V. (1991). *A&A* **242**, 125
- Ergma, E. and van den Heuvel, E. P. J. (1998). *A&A* **331**, L29
- Ergma, E., Sarna, M. J. and Antipova, J. (1998). *MNRAS* **300**, 352
- Faulkner, J. (1971). *ApJ* **170**, L99
- Finn, L. S. (1997), in *Gravitation & Cosmology*, eds. S. Dhurandhar and T. Padmanabhan (Dordrecht, Kluwer) p. 95  
(1998). *Phys. Rev.* **D53**, 2878
- Flannery, B. P. and van den Heuvel, E. P. J. (1975). *A&A* **39**, 61
- Fryer, C. L. (1999). *ApJ* **522**, 413
- Fryer, C. L., Woosley, S. E. and Hartmann, D. H. (1999). *ApJ* **526**, 152
- Fryxell, B. A. and Taam, R. E. (1988). *ApJ* **335**, 862
- Galloway, D. K., Chakrabarty, D., Morgan, E. H. and Remillard, R. A. (2002). *ApJ* **576**, L137
- Geppert, U. and Urpin, V. (1994). *MNRAS* **271**, 490
- Ghosh, P. and Lamb, F. K. (1979). *ApJ* **234**, 296
- Giacconi, R., Gursky, H., Paolini, F. R. and Rossi, B. B. (1962). *Phys. Rev. Lett.* **9**, 439
- Habets, G. M. H. J. (1986). *A&A* **167**, 61
- Han, Z., Podsiadlowski, P. and Eggleton, P. P. (1994). *MNRAS* **270**, 121  
(1995). *MNRAS* **272**, 800
- Han, Z., Podsiadlowski, P., Maxted, P. F. L., *et al.* (2002). *MNRAS* **336**, 449

- Hills, J. (1983). *ApJ* **267**, 322
- Heuvel, E. P. J. van den (1975). *ApJ* **198**, L109  
 (1994), in *Interacting Binaries*, Saas-Fee course 22 (Heidelberg, Springer) p. 263  
 (2003). *Nature* **426**, 504  
 (2004). *Science* **303**, 1143
- Heuvel, E. P. J. van den and Heise, J. (1972). *Nature – Physical Science* **239**, 67
- Heuvel, E. P. J. van den and de Loore, C. (1973). *A&A* **25**, 387
- Heuvel, E. P. J. van den and Rappaport, S. A. (1987), in *Physics of Be-stars*, Proc. IAU Colloq. 92 (Cambridge University Press) p. 291
- Heuvel, E. P. J. van den and van Paradijs, J. (1988). *Nature* **334**, 227
- Hulse, A. R. and Taylor, J. H. (1975). *ApJ* **195**, L51
- Iben, Jr. I. and Livio, M. (1993). *PASP* **105**, 1373
- Illarionov, A. F. and Sunyaev, R. A. (1985). *A&A* **39**, 185
- Iwamoto, K., Mazzali, P. A., Nomoto, K., *et al.* (1998). *Nature* **395**, 672
- Joss, P. C., Rappaport, S. A. and Lewis W. (1987). *ApJ* **319**, 180
- Kalogera, V. and Webbink, R. F. (1996). *ApJ* **458**, 301  
 (1998). *ApJ* **493**, 351
- Kalogera, V., Narayan, R., Spergel, D. N. and Taylor, J. H. (2001). *ApJ* **556**, 340
- Kalogera, V., Kim, C., Lorimer, D. R., *et al.* (2004). *ApJ* **601**, L179
- Kaspi, V. M., Bailes, M., Manchester, R. N., *et al.* (1996). *Nature* **381**, 584
- King, A. R. and Begelman, M. C. (1999). *ApJ* **519**, 169
- King, A. R. and Ritter, H. (1999). *MNRAS* **309**, 253
- Kippenhahn, R. and Weigert, A. (1967). *Z. Astrophys.* **65**, 251  
 (1990). *Stellar Structure and Evolution* (Heidelberg, Springer)
- Kirk, J. G. and Trümper, J. E. (1983), in *Accretion Driven Stellar X-ray Sources*, eds. W. H. G. Lewin and E. P. J. van den Heuvel (Cambridge University Press) p. 216
- Konar, S. and Bhattacharya, D. (1997). *MNRAS* **284**, 311
- Kraft, R. P. (1967). *ApJ* **150**, 551
- Landau, L. D. and Lifshitz, E. (1958). *The Classical Theory of Fields* (Oxford, Pergamon Press)
- Lee, C. H., Brown, G. E. and Wijers, R. A. M. J. (2002). *ApJ* **575**, 996
- Lewin, W. G. H. and Joss, P. C. (1983), in *Accretion Driven Stellar X-ray Sources*, eds. W. H. G. Lewin and E. P. J. van den Heuvel (Cambridge University Press) p. 41
- Liu, Q. Z., van Paradijs, J. and van den Heuvel, E. P. J. (2000). *A&AS* **147**, 25
- Lyne, A. G. and Lorimer, D. R. (1994). *Nature* **369**, 127
- Lyne, A. G., Burgay, M., Kramer, M., *et al.* (2004). *Science* **303**, 1153
- MacFadyen, A. I., Woosley, S. E. and Heger, A. (2001). *ApJ* **550**, 410
- Manchester, R. N. and Taylor, J. H. (1977). *Pulsars* (San Francisco, Freeman)
- Maraschi, L., Treves, A. and van den Heuvel, E. P. J. (1976). *Nature* **259**, 292
- Markwardt, C. B., Smith, E. and Swank, J. H. (2003). *The Astronomer's Telegram* **122**
- Matsuda, T., Ishii, T., Sekino, N., *et al.* (1992). *MNRAS* **255**, 183
- Maxted, P. F. L., Heber, U., Marsh, T. R. and North, R. C. (2001). *MNRAS* **326**, 1391
- McClintock, J. E. and Remillard, R. A. (1986). *ApJ* **308**, 110
- Mestel, L. (1984), in *Cool Stars, Stellar Systems, and the Sun*, eds. S. L. Baliunas, L. Hartmann (Berlin, Springer) p. 49
- Mirabel, I. F., Mignami, R., Rodrigues, I., *et al.* (2002). *A&A* **395**, 595
- Nelemans, G. and van den Heuvel, E. P. J. (2001). *A&A* **376**, 950
- Nelemans, G., Tauris, T. M. and van den Heuvel, E. P. J. (1999). *A&A* **352**, L87
- Nomoto, K. (1984). *ApJ* **277**, 791
- Novikov, I. D. and Zel'Dovitch, Y. B. (1966). *Nuova Cimento Sup.* **4**, 810
- Nugis, T. and Larmers, H. J. G. L. M. (2000). *A&A* **360**, 227
- Orosz, J. A., Jain, R. K., Bailyn, C. D., *et al.* (1998). *ApJ* **499**, 375
- Orosz, J. A., Kuulkers, E., van der Klis, M., *et al.* (2001). *ApJ* **555**, 489
- Ostriker J. P. (1976), in *Structure and Evolution of Close Binary Systems*, eds. P. P. Eggleton *et al.* (Dordrecht, Reidel) p. 206
- Paczynski B. (1971). *Acta Astron.* **21**, 1  
 (1976), in *Structure and Evolution of Close Binary Systems*, eds. P. P. Eggleton *et al.* (Dordrecht, Reidel) p. 75

- Paradijs, J. van (1996). *ApJ* **464**, L139
- Parker, E. N. (1955). *ApJ* **121**, 491
- Peters, P. C. (1964). *Phys. Rev* **136**, B1224
- Pfahl, E., Podsiadlowski, P., Rappaport, S. A. and Spruit, H. (2002). *ApJ* **574**, 364
- Podsiadlowski, P. (1991). *Nature* **350**, 136
- Podsiadlowski, P. and Rappaport, S. A. (2000). *ApJ* **529**, 946
- Podsiadlowski, P., Rappaport, S. A. and Pfahl, E. (2002). *ApJ* **565**, 1107
- Podsiadlowski, P., Rappaport, S. A. and Han, Z. (2003). *MNRAS* **340**, 1214
- Pols, O. R., Tout, C. A., Eggleton, P. P. and Han, Z. (1995). *MNRAS* **274**, 964
- Pols, O. R., Schröder, K. P., Hurley, J. R., *et al.* (1998). *MNRAS* **298**, 525
- Portegies-Zwart, S. F. and McMillan, S. L. W. (2000). *ApJ* **528**, L17
- Pringle, J. E. (1981). *ARA&A* **19**, 137
- Pyllyser, E. and Savonije, G. J. (1988). *A&A* **191**, 57  
(1989). *A&A* **208**, 52
- Radhakrishnan, V. and Srinivasan, G. (1982). *Current Science* **51**, 1096
- Rappaport, S. A., Verbunt, F. and Joss, P. C. (1983). *ApJ* **275**, 713
- Rappaport, S. A., Podsiadlowski, P., Joss, P. C., *et al.* (1995). *MNRAS* **273**, 731
- Refsdal, S. and Weigert, A. (1971). *A&A* **13**, 367
- Reimers, D. (1975), in *Problems in Stellar Atmospheres and Envelopes*, eds. B. Baschek, W. H. Kegel and G. Traving. (New York, Springer) p. 229
- Reimers, D. and Koester, D. (1988). *ESO Messenger* **54**, 47
- Rucinski, S. M. (1983). *Observatory* **103**, 280
- Ruderman, M. A. (1998), in *The Many Faces of Neutron Stars*, eds. R. Buccheri, J. van Paradijs and A. Alpar. (Dordrecht, Kluwer) p. 77
- Ruderman, M. A., Shaham, J. and Tavani, M. (1989). *ApJ* **336**, 507
- Salpeter, E. E. (1964). *ApJ* **140**, 796
- Savonije, G. J. (1978). *A&A* **62**, 317  
(1983), in *Accretion Driven Stellar X-ray Sources*, eds. W. H. G. Lewin and E. P. J. van den Heuvel (Cambridge University Press) p. 343  
(1987). *Nature* **325**, 416
- Schaller, G., Schaerer, D., Meynet, G. and Maeder, A. (1992). *A&AS* **96**, 269
- Schreier, E., Levinson, R., Gursky, H., *et al.* (1972). *ApJ* **172**, L79
- Schutz, B. F. (1986). *Nature* **323**, 310
- Shaham, J. (1992), in *X-ray Binaries and Recycled Pulsars*, eds. E. P. J. van den Heuvel and S. A. Rappaport. (Dordrecht, Kluwer) p. 375
- Shklovskii, I. (1967). *ApJ* **148**, L1
- Sipior, M. S. and Sigurdsson, S. (2002). *ApJ* **572**, 962
- Skumanich, A. (1972). *ApJ* **171**, 565
- Slettebak, A. (1988). *Publ. Astron. Soc. Pac.* **100**, 770
- Smarr, L. L. and Blandford, R. D. (1976). *ApJ* **207**, 574
- Soberman, G. E., Phinney, E. S. and van den Heuvel, E. P. J. (1997). *A&A* **327**, 620
- Sonderblom, D. R. (1983). *ApJS* **53**, 1
- Soria, R., Wu, K., Page, M. J. and Sakelliou, I. (2001). *A&A* **365**, L273
- Spruit, H. C. and Ritter, H. (1983). *A&A* **124**, 267
- Srinivasan, G. and van den Heuvel, E. P. J. (1982). *A&A* **108**, 143
- Stepien, K. (1995). *MNRAS* **274**, 1019
- Sutantyo, W. (1975). *A&A* **41**, 47
- Taam, R. E. (1983). *ApJ* **270**, 694
- Taam, R. E. and Fryxell, B. A. (1988). *ApJ* **327**, L73
- Taam, R. E. and van den Heuvel, E. P. J. (1986). *ApJ* **305**, 235
- Taam, R. E. and Sandquist, E. L. (2000). *ARA&A* **38**, 113
- Tauris, T. M. (1996). *A&A* **315**, 453  
(2001), in *Evolution of Binary and Multiple Star Systems*, eds. P. Podsiadlowski *et al.* (ASP Conf. Vol. 229)
- Tauris, T. M. and Dewi, J. D. M. (2001). *A&A* **369**, 170
- Tauris, T. M. and Konar, S. (2001). *A&A* **376**, 543
- Tauris, T. M., van den Heuvel, E. P. J. and Savonije, G. J. (2000). *ApJ* **530**, L93

- Tauris, T. M. and Savonije, G. J. (1999). *A&A* **350**, 928
- Tauris, T. M. and Savonije, G. J. (2001), in *The Neutron Star–Black Hole Connection*, eds. C. Kouveliotou *et al.* (NATO ASI, Dordrecht, Kluwer)
- Tauris, T. M. and Takens, R. (1998). *A&A* **330**, 1047
- Tavani, M. (1992), in *X-ray Binaries and Recycled Pulsars*, eds. E. P. J. van den Heuvel and S. A. Rappaport (Kluwer, Dordrecht) p. 387
- Taylor, J. H. and Weisberg, J. M. (1989). *ApJ* **345**, 434
- Terquem, C., Papaloizou, J. C. B., Nelson, R. P. and Lin, D. N. C. (1998). *ApJ* **502**, 588
- Thorne, K. S. (2001). LIGO Document Number P-000024-00-D
- Thorsett, S. E. and Chakrabarty, D. (1999). *ApJ* **512**, 288
- Tutukov, A. V. and Yungelson, L. R. (1973). *Nauchnye Informatsii* **27**, 70
- Verbunt, F. and Phinney, E. S. (1995). *A&A* **296**, 709
- Verbunt, F. and van den Heuvel, E. P. J. (1995), in *X-ray Binaries*, eds. W. H. G. Lewin, J. van Paradijs and E. P. J. van den Heuvel (Cambridge University Press)
- Verbunt, F. and Zwaan, C. (1981). *A&A* **100**, L7
- Vilhu, O. and Walter, F. M. (1987). *ApJ* **321**, 958
- Voss, R. and Tauris, T. M. (2003). *MNRAS* **342**, 1169
- Webbink, R. F. (1984). *ApJ* **277**, 355
- Webbink, R. F., Rappaport, S. A. and Savonije, G. J. (1983). *ApJ* **270**, 678
- Webster, B. L. and Murdin, P. (1972). *Nature* **235**, 37
- Weidemann, V. (1990). *ARA&A* **28**, 103
- Wellstein, S. and Langer, N. (1999). *A&A* **350**, 148
- Wijnards, R. and van der Klis, M. (1998). *Nature* **394**, 344
- Witte, M. G. (2001). Ph.D. thesis, University of Amsterdam
- Witte, M. G. and Savonije, G. J. (1999). *A&A* **350**, 129
- Wolszczan, A. (1994). *Science* **264**, 538
- Woosley, S. E. and Weaver, T. A. (1995). *ApJS* **101**, 181
- Woosley, S. E., Langer, N. and Weaver, T. A. (1995). *ApJ* **448**, 315
- Zel'Dovitch, Y. B. (1964). *Soviet Physics Doklady* **9**, 195
- Zel'Dovitch, Y. B. and Guseinov, O. (1966). *ApJ* **144**, 840
- Zel'Dovitch, Y. B. and Novikov, I. D. (1964). *Doklady Akademii Nauk SSSR* **158**, 811

